1-1-1967

A re-examination of the kinetics of dissolution of tin in hydrochloric acid.

David S.P. Poa
University of Windsor

A RE-EXAMINATION OF THE KINETICS OF DISSOLUTION OF TIN IN HYDROCHLORIC ACID

A Thesis
Submitted to the Faculty of Graduate Studies through the Department of Chemical Engineering in Partial Fulfilment of the Requirements for the Degree of Master of Applied Science at the University of Windsor

by

David S.P. Poa

Windsor, Ontario
1967

ACT 3031

APPROVED BY: Robert A. Hager

Alex Smyth

Roger J. Thibert

177760

ABSTRACT

A kinetic study of the dissolution of tin in hydrochloric acid solutions in the presence and absence of oxygen has been made.

It has been found that the tin dissolution process in aerated hydrochloric acid solutions appears to occur through three simultaneous reactions, hydrogen evolution, oxygen depolarization, and an autocatalytic reaction.

Over the range of conditions studied the dissolution rate may be expressed by the empirical equation:

$$\frac{d}{dt}[Sn] = 5.31 \times 10^{-7} \frac{A}{V} [HCl]^{0}[v]^{0.98} e^{-\frac{3060}{RT}}$$

$$+ \; 2.88 \times 10^{-5} \frac{A}{V} [HCl]^{0}[v]^{0.98}[P_{O_2}]^{1/2} e^{-\frac{3660}{RT}}$$

$$+ \; 1.25 \times 10^{-1} \frac{[A]^{1/2}}{V} [HCl]^{0}[v]^{n}[P_{O_2}]^{1/2}[Sn]^{1/2} e^{-\frac{5440}{RT}}$$

in which the third term (autocatalytic) applies only after an elapsed time of 30 minutes.

Low temperature coefficients, and significant effects of peripheral velocity and turbulence indicate that diffusional processes are involved in the controlling step. The dependence of the dissolution rate on the square root of the oxygen partial pressure is indicative of a dissociative adsorption of oxygen on the metal surface.

ACKNOWLEDGMENTS

The author wishes to express his sincere gratitude to Dr. A.W. Gnyp for his able guidance, constructive criticisms, and encouragement throughout this work.

Thanks are expressed to Mr. Halil Parlar for machining the tin samples and assistance in setting up the apparatus.

The financial assistance offered by the National Research Council has been appreciated.

TABLE OF CONTENTS

		Page
ABSTRACT		iii
ACKNOWLEDGMENTS		iv
TABLE OF CONTENTS		v
LIST OF TABLES		vii
LIST OF FIGURES		viii
Chapter		
I.	INTRODUCTION	1
II.	LITERATURE REVIEW	2
	A. Kinetic Studies on Metal Dissolution	2
	B. General Review of Studies on Tin Corrosion	2
	C. Hydrodynamic Factors in the Dissolution of Metals	5
	D. The Analysis of Tin	6
III.	EXPERIMENTAL WORK	8
	A. Materials	8
	B. Apparatus	8
	C. Procedure	10
IV.	GENERAL THEORY OF METAL DISSOLUTION	12
V.	EXPERIMENTAL RESULTS AND DISCUSSION	22
	A. General Behavior of Tin Dissolution in HCl Solutions	22
	B. Rate Dependence on Tin Ion Concentration	22
	C. Rate Dependence on Peripheral Velocity	25
	D. Rate Dependence on Temperature	29
	E. Rate Dependence on Surface Area and Corroding Solution Volume	34
	F. Effect of Hydrochloric Acid Concentration	34
	G. Rate Dependence on Oxygen Concentration	38
	H. The Effect of Hydrodynamic Factors	40
	I. Mechanism of Tin Dissolution in Hydrochloric Acid	42
	J. Empirical Equation for Tin Dissolution in Hydrochloric Acid	45
VI.	CONCLUSIONS	49

		Page
APPENDIX I.	Polarographic Determination of Tin Concentration	51
APPENDIX II.	Data of Tin Dissolution	53
APPENDIX III.	Nomenclature	70
REFERENCES		71
VITA AUCTORIS		73

LIST OF TABLES

Table		Page
I.	Effect of Hydrochloric Acid Concentration on Dissolution Rate	38
II.	Evaluation of Velocity Constant k_1^o for Hydrogen Evolution	46
III.	Evaluation of Velocity Constant k_2^o for Oxygen Depolarization	47
IV.	Evaluation of Velocity Constant k_3^o for autocatalytic Reaction	47

LIST OF FIGURES

Figure		Page
1.	Arrangement of Apparatus	9
2.	A Two-dimensional Model of Polished Surfaces on an Atomic Scale	13
3.	Dissolution of Metal in Acidic Media	21
4.	Dissolution of Tin in Hydrochloric Acid	23
5.	Half-order Dependence for Autocatalytic Reaction	24
6A.	Dissolution as Function of Peripheral Velocity (hydrogen evolution)	26
6B.	Dissolution as Function of Peripheral Velocity (oxygen depolarization)	27
7.	Dissolution as Function of Peripheral Velocity (autocatalytic reaction)	28
8.	Dissolution as Function of Temperature (H_2 evolution)	30
9.	Dissolution as Function of Temperature (oxygen depolarization)	31
10.	Dissolution as Function of Temperature (autocatalytic reaction)	32
11.	Activation Energy as Function of Sample Diameter (autocatalytic reaction)	33
12.	Dissolution as Function of Surface Area (H_2 evolution and oxygen depolarization)	35
13.	Dissolution as Function of A/V (H_2 evolution and oxygen depolarization)	36
14.	Dissolution as Function of Surface Area (autocatalytic reaction)	37
15.	Dissolution as Function of A/V (autocatalytic reaction)	37
16A.	Effect of Oxygen Concentration on Oxygen Depolarization	39

Figure Page

16B. Effect of Oxygen Concentration on Autocatalytic Reaction 39

17. Effect of Hydrodynamic Factors on Hydrogen Evolution 41

18. Effect of Hydrodynamic Factors on Oxygen Depolarization 41

19. Effect of Hydrodynamic Factors on Autocatalytic Reaction 41

20. Calibration Curve for Sargent Model XV Polarograph 52

CHAPTER I

INTRODUCTION

Research and development in the field of corrosion science have been stimulated by problems related to advances in technology, and facilitated by parallel advances in other fields of science. Despite the progress which has been made, however, our approaches to the prevention of corrosion in practice are empirical. We still do not have principles which will allow us to forecast the behavior of a given material in a given situation. Our inability to deal with corrosion on a more rational basis stems largely from our great ignorance of the details of the mechanisms involved.

Several investigations have been done on the mechanism and kinetics of the dissolution of copper[8,22,23], tin[24] and titanium[4]. It has been shown that over a wide range of conditions the dissolution of these metals in air-saturated acidic media is autocatalytic.

The purpose of the present study was two-fold: (1) to attempt to determine the rate-determining step and make a further study of the mechanism and kinetics of the dissolution of tin in hydrochloric acid solutions with the hope of providing a more reasonable description clarifying the way by which this metal is destroyed, (2) to study the role of hydrodynamic factors near the metal surface on the dissolution process.

This project was based partly on the fundamental work of Lui[24] who studied the dissolution of tin in hydrochloric acid solutions.

CHAPTER II

LITERATURE REVIEW

A. Kinetic Studies on Metal Dissolution

Lu and Graydon[22,23] studied the kinetics and mechanism of copper dissolution in aqueous ammonium hydroxide and aqueous sulfuric acid solutions. Weeks and Hills[29] investigated the initial corrosion rate of copper in HCl solutions. Their work was extended by Gnyp[8]. Later, systematic researches on the dissolution kinetics of brass were done by Kagetsu and Graydon[11] and Bumbulis and Graydon[6], and titanium by Bodner[4]. The above investigators studied the rate of metal dissolution in aerated solutions as a function of temperature, oxygen partial pressure, rotational speed, sample surface area, corroding solution volume and acid concentration. Over a wide range of conditions, all of them found an autocatalytic effect, with dissolution rate increasing with increasing metal ion concentration in solution.

B. General Review of Studies on Tin Corrosion

As early as 1813, the dissolution of tin in acid solutions was examined by Berzelius[2,3]. According to his report, tin dissolves in hydrochloric and sulfuric acid solutions in the stannous form with the evolution of hydrogen gas.

Evans[7] reported that tin, which stands immediately below hydrogen in the table of normal potentials, liberates hydrogen from dilute HCl only very slowly. Here it is the high overpotential of hydrogen evolution on a tin surface which is responsible for the sluggish reaction.

Whitman and Russel[30] studied the difference in the rate of corrosion of tin in moderately concentrated acids at room temperature in the presence and absence of oxygen. They showed that, in most cases, oxidizing agents act as depolarizers, and if added to acids, will increase the attack on tin. In the absence of air or other oxidizing agents, tin was very resistant to dilute acids. This is because tin has a high hydrogen overpotential, and it quickly becomes polarized by hydrogen which prevents the flow of current that accompanies corrosion.

Kohman and Sanborn[14] reported that, in air-free solutions, tin is depolarized by increasing the temperature of the solution, and hydrogen evolution occurs. The effect of temperature on the corrosion of tin in acid solutions was also investigated by Khitrav and Shotalova[12]. The rate of tin corrosion in 1-7 M solutions of hydrochloric acid and sulfuric acid was observed to increase with increasing temperature. In the 0-80°C range the rate obeyed the van't Hoff and Arrhenius Laws. The rate of diffusion also increased with increase in temperature but not as rapidly as the corrosion rate. The increase of corrosion rate with increasing temperature is associated with a fall in hydrogen overpotential, decrease in polarization, decrease in viscosity of the solution and destruction of protective films.

An instructive case of localized corrosion of tin, investigated by Hoar[10], showed that the salts of tin are strongly hydrolyzed, and in a neutral solution anodic attack at a weak spot on the air formed film covering the metal will not cause tin cations to pass into the liquid, but rather cause an increase in the film-thickness by deposition of oxide and hydroxide. After a certain time the accumulated acidity at these

points apparently became sufficient for the formation of soluble stannous ions, which ruin the film so that break-down occurred with the formation of the black spots. Britton and Michael[5] studied the local corrosion of tin in chloride solutions. Their results showed that the time elapsing before local corrosion begins is affected by surface conditions. Local corrosion is initiated and accelerated by crevices resulting from surface defects or by contact of the metal with another surface. The blackness of the spots, according to Britton, is probably due to the absence of reflection from the locally roughened surface.

Hagymas and Quintin[9] studied the corrosion of tin in sulfuric acid. In 0.1 to 1.0 M solutions the hydrogen overvoltage on the tin electrode did not vary with acid concentration. Kahman and Sanborn[15] also reported that there was no apparent influence of acid concentration on the corrosion of tin in air-free solutions.

Marshakov, Ugai and Vigdorovich[25] reported that in acidic media the corrosion of magnesium-tin alloys is uniform in character. The specimen surface becomes coated with a gray film which does not adhere firmly to the metal. Chemical analysis showed it to be almost pure tin.

Probably the most extensive and systematic study on the dissolution rate of tin was done by Lui[24]. He reported that over a wide range of conditions the dissolution of tin in hydrochloric acid solutions proceeds in two autocatalytic stages with the rate during each stage being dependent on the square root of the stannic ion concentration in the corroding solution.

C. Hydrodynamic Factors in the Dissolution of Metals

Studies on the rates of heterogeneous processes in liquids began with the simplest problem in diffusion kinetics, namely the dissolution of solids in liquids. Upon analysis, the experimental data collected by Shchukorev[27] yielded the following empirical equation for dissolution:

$$Q = k\ (C_s - C_o)\ S$$

where Q is the amount of material dissolved per unit time, S is the surface area of the dissolving body, C_s is the concentration of a saturated solution, C_o is the concentration of the bulk solution at a given instant, and k is a proportional constant.

Further studies, primarily by Nernst[26], showed that k is proportional to D, the diffusion coefficient of the substance in the liquid. Thus the expression for Q may be written in the form:

$$Q = \frac{D\ (C_s - C_o)\ S}{\delta}$$

It has been found that under ordinary mixing conditions, the quantity δ has a magnitude of 10^{-2} to 10^{-4} cm., which is extremely small compared to the dimension of the usual reaction vessels. This led Nernst to assume that the δ represents the thickness of the layer across which the diffusion occurs in a moving liquid. According to the Nernst Theory, there is a thin layer of static liquid immediately adjacent to the surface of the solid body , a layer through which diffusion of the reacting molecules takes place. Beyond this layer, the concentration in the bulk of the solution is constant because of the liquid motion. The symbol δ is termed the thickness of the Nernst diffusion layer. Experimental

determinations have shown that, δ, as a function of velocity, has the form:

$$\delta = \frac{1}{v^n}$$

where v is the velocity of the moving liquid. The value of n varies from 1/2 to 1. In general, the rate of diffusion-controlled reactions can be largely increased by agitating the liquid with stirrers or rotating the solid body of dissolving substances because the diffusion coefficient in a moving, turbulent medium is much larger than that in a static medium.

Levich[17] was the first to formulate the diffusion factor for a rotating specimen in solution. He showed that the diffusional flux of mass in a turbulent liquid may be represented by an equation in the form:

$$J = (D + D_{turb}) \frac{\partial c}{\partial y}$$
$$= (D + \beta \overline{\ell v}) \frac{\partial c}{\partial y}$$

where ℓ is the scale of the eddies and v is the peripheral velocity. The bar above the ℓv indicates the average value; β is a constant. The large value of D_{turb} ensures a virtually constant concentration of the solution down to very small distance from the reaction surface.

D. The Analysis of Tin

The analysis of tin by the polarographic method has been well developed by Lingane[18,19,20]. The reduction of stannous tin to the metallic tin produces defined waves from 1M HCl, with a half-wave potential of -0.47v vs S.C.E. when 0.01 per cent gelatin is present as a suppressor. Chlorostannate complex ion also produces a well developed doublet wave. The first wave results from the reduction of the chlorostannate ion to the chlorostannite ion, and the second wave corresponds

to complete reduction to the metal. A supporting electrolyte consisting of 4M NH_4Cl, 1M HCl, and 0.005 per cent gelatin was used as the maximum suppressor. The half-wave potential of the first wave is -0.25v and that of the second is -0.52v vs S.C.E. in the previous described conditions. The first wave is not fully developed before the second stage of reduction begins. Measurement of the second wave for routine analysis is recommended by Lingane.

CHAPTER III

EXPERIMENTAL WORK

A. Materials

The Analar grade tin bars used in this study were supplied by British Drug House Ltd. The purity of metal was 99.92 per cent tin. The exact analysis according to the manufacturer showed 0.01 per cent lead, 0.0025 per cent copper, 0.002 per cent bismuth, 0.002 per cent iron, 0.04 per cent total foreign metals, 0.0001 per cent arsenic, and 0.025 per cent antimony.

The tin bars, originally 1.02 cm. in diameter, were melted and remoulded into 1.91 and 2.54 cm. diameter bars under argon gas in a vacuum furnace. Cylinders of 0.915 to 2.42 cm. in diameter, 0.48 to 1.27 cm. in length, with a concentric hole to fit onto a rotating shaft were machined from these remoulded tin bars.

Hydrochloric acid and all other reagents used were of analytical grade. Dilute HCl solutions were made with distilled water.

B. Apparatus

The apparatus used for this investigation is shown in Figure 1.

The reaction cell consisted of a specially designed jacketed vessel fabricated from two Pyrex beakers. Water was forced through the shell by means of a pump from a constant temperature bath. The top of the reaction vessel was covered with a Plexiglas plate holding up to three radially mounted baffle plates designed to prevent vortex formation

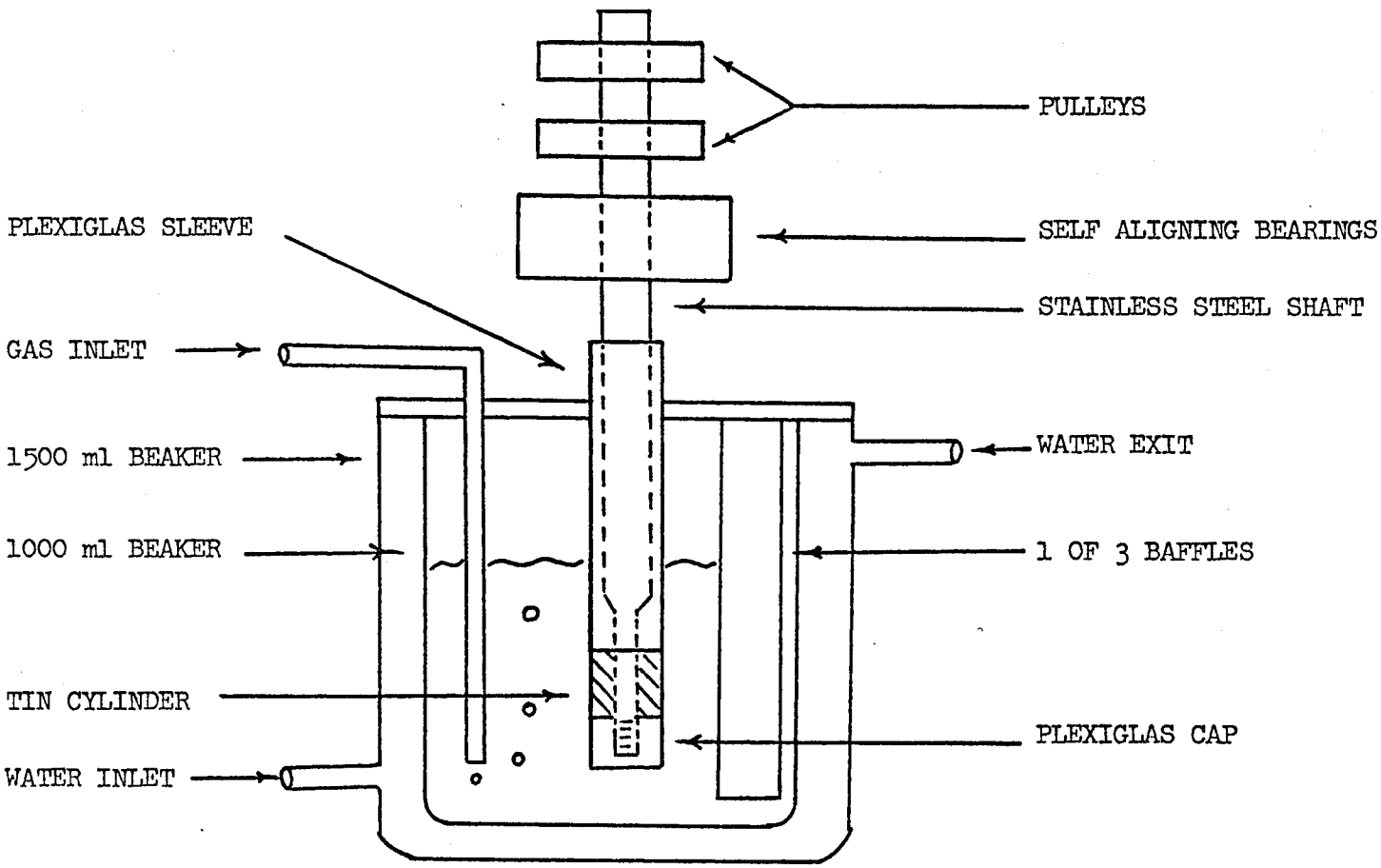

FIGURE 1. ARRANGEMENT OF APPARATUS

when the shaft was rotated at high speeds.

The cylindrical tin samples were rotated on a stainless steel shaft. The ends of the tin cylinders were protected from the corroding medium by Plexiglas sleeves and a cap screwed tightly at the end. The shaft was driven by a Type 7 HM Hoover vacuum cleaner motor whose speed was controlled by a autotransformer and a constant voltage regulator. Shaft speeds were measured by means of a Type 1531-A Strobotac produced by the General Radio Corporation.

C. Procedure

A typical experiment was run by pouring a measured volume of HCl solution into the reaction vessel and flushing the liquid with appropriate gas for approximately 20 minutes before start-up. During the test period the hydrochloric acid solution was kept saturated with air, nitrogen, or oxygen. Losses of hydrochloric acid were minimized by passing the gases through a series of washing bottles containing HCl solution of the same concentration as in the reaction vessel. All wash bottles were kept at the same temperature as the corroding solution.

The tin cylinders, polished manually to 3/0 emery paper smoothness (average surface roughness less than 20 microinches), were washed initially with distilled water and dried with filter paper, then washed with acetone for degreasing, and finally rewashed with distilled water. After each run, the tin cylinders were washed and dried. A check on the material balance was maintained by weighing the clean dry tin cylinders before and after each run.

An appropriately sized sample of the corroding solution was withdrawn for routine polarographic analysis at convenient intervals of

time. For every sample of corroding solution withdrawn, an equal volume of HCl solution of the same concentration was added to the vessel to eliminate solution volume change during the corrosion run.

CHAPTER IV

GENERAL THEORY OF METAL DISSOLUTION

The dissolution of metals in acidic media is an electrochemical process. However, the electrochemical processes are greatly complicated by the chemical interactions of the surface atoms of the metal with the components of the solution.

In deaerated acid solutions, the basic dissolution process of any metal M, which displaces hydrogen from acid solution, can be represented by the following anodic and cathodic reactions:

(i) Anode:

$$M \rightarrow M^{++} + 2e$$

Assuming formation of divalent metallic ions.

(ii) Cathode:

(iia) The discharge of hydrogen ions, generally represented by

$$H^{+} + e = H$$

(Perhaps more accurately written as: $H_3O^{+} + e = H + H_2O$)

(iib) The formation of molecular hydrogen from atomic hydrogen, either by

$$H + H = H_2$$

or by

$$H + H^{+} + e = H_2$$

(The last reaction is perhaps more accurately written as

$$H^{+} + H_3O^{+} + e = H_2 + H_2O)$$

The above equations are oversimplified net results of the

dissolution process of metals in acidic solutions. The details of the mechanisms involved should be considered if we intend to deal with corrosion problems on a more rational basis.

We customarily treat a metal as a homogeneous continuum. Now on an atomic scale a metal is decidedly not continuous, and it is on exactly this scale that the individual acts of corrosion occur, because corrosion is essentially a process in which the atoms of a metal are removed one at a time therefore in order to reach our goal of understanding and controlling corrosion we need greatly increased knowledge of the detailed atomic mechanisms involved.

Firstly in corrosion studies we will be concerned with surfaces polished by different procedures. Such surfaces will not be uniform but will contain many different types of sites with different chemical or physical properties. A two-dimensional model of such surfaces on an atomic scale is shown in Figure 2.

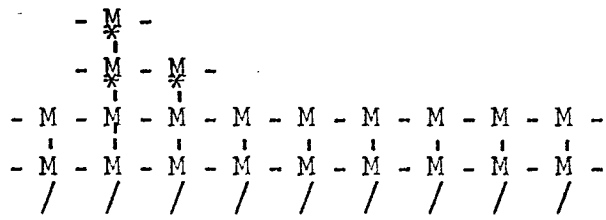

FIGURE 2.

Some surface atoms may be held by one bond, others by two, three, and so on. There may thus be many different degrees of interactions with a metal surface. The most active points will be occupied first and with the largest heat of adsorption. Also the surface energy of a metal may

vary from one locality to another because of the exposure of various crystal planes.

The points where corrosion starts are generally determined by surface defects which may represent places where the atoms are most loosely correlated to the metal matrix (such as M^* in Figure 2). Because of their unsatisfied binding energy conditions, it is easier for them to attract and hold components from the solution. These sites also represent places where the atoms are disarrayed and therefore escape easily into the solution. For example, the corrosion of a metal crystal containing dislocations often results in the formation of etch pits where the dislocations meet the surface.

The dissolution process can now be described in terms of the following elementary stages:

1. First, when a strong acid such as hydrochloric acid dissolve in water, we have

$$HCl + H_2O \rightarrow H_3O^+ + Cl^-$$

The bulk solution, therefore, consists of water, the hydrogen ions, and the chloride ions. In general, the contact between two non-miscible phases is accompanied by an increased concentration of the fluid phase close to the interface. This tendency leads to the formation of a "diffusion layer". Therefore, when a metal sample is placed in the acidic solution, the hydrogen ions will diffuse through this layer, from the bulk solution to the metal-solution interface

$$H^+_{bulk} \rightarrow H^+_i$$

where H^+_i represents a hydrogen ion at the metal-solution interface.

2. The adsorption of hydrogen ions on the metal surface

$$H_i^+ + \underset{*}{M} \rightleftarrows \underset{*}{M}\text{-}H_s^+$$

where $\underset{*}{M}\text{-}H_s^+$ denotes a hydrogen ion adsorbed on an active site on the metal surface:

3. Discharge of adsorbed hydrogen ions by virtue of electron transfer through the metal:

(3a) Electrons transferred from a neighbouring vacant site on the surface

$$\begin{array}{ccccccccccccc} & & H^+ & & & & H^+ & & & & H & & H \\ & & | & & & & | & & & & | & & | \\ -\underset{*}{M} & - & M & - & \underset{*}{M} & - & M & - & \underset{*}{M} & - & \overset{++}{M} & - & M & - & \underset{*}{M} & - \end{array} \rightarrow \begin{array}{ccccccccccccc} & & & & & & & & & & & & \\ & & & & & & & & & & & & \\ -\underset{*}{M} & - & M & - & \underset{*}{M} & - & M & - & \overset{++}{\underset{*}{M}} & - & M & - & \underset{*}{M} & - \end{array}$$

(3b) Electrons transferred directly from the surface atoms on which adsorption occured

$$\underset{*}{M}\text{-}H_s^+ \rightarrow \overset{+}{\underset{*}{M}}\text{-}H_s$$

4. Formation of molecular hydrogen from atomic hydrogen, by one of the following possible modes:

(4a)

$$\begin{array}{ccccccccccccc} & & H & & & & H & & & & & & H_2 \\ & & | & & & & | & & & & & & | \\ -\underset{*}{M} & - & M & - & \overset{++}{\underset{*}{M}} & - & M & - & \underset{*}{M} & - & & & \underset{*}{M} & - \end{array} \rightarrow \begin{array}{ccccccccccccc} & & & & & & & & & & & & \\ & & & & & & & & & & & & \\ -\underset{*}{M} & - & M & - & \overset{++}{\underset{*}{M}} & - & M & - & \underset{*}{M} & - & & & \underset{*}{M} & - \end{array}$$

(4b) $$2(\overset{+}{\underset{*}{M}}\text{-}H_s) \rightarrow \overset{++}{\underset{*}{M}}_s + \underset{*}{M}\text{-}H_{2_s}$$

(4c) The so-called "electrochemical" or ion atom reaction

$$\overset{+}{\underset{*}{M}}\text{-}H_s + H_i^+ \rightarrow \overset{++}{\underset{*}{M}}\text{-}H_{2_s}$$

5. Formation of metallic hydride through a series of successive stages of adsorption and discharge

$$\underset{*}{M}\text{-}H_s^+ + H_i^+ \rightarrow H_s^+\text{-}\underset{*}{M}\text{-}H_s^+$$

$$H_s^+\text{-}\underset{*}{M}\text{-}H_s^+ + H_i^+ \rightarrow \begin{array}{c} H^+ \\ | \\ s \end{array}$$

$$H_s^+\text{-}\underset{*}{M}\text{-}H_s^+$$

.....

$$H_s^+\text{-}\overset{*}{M}\text{-}H_s^+ + \overset{*}{M} \rightarrow \overset{*}{M}\text{-}H_{2_s} + \overset{*}{M}_s^{++}$$

$$H_s^+\text{-}\overset{*}{M}\text{-}H_s^+ \quad (H_s^+) + \overset{*}{M} \rightarrow \overset{*}{M}\text{-}H_{3_s} + \overset{*}{M}_s^{+++}$$

.....

6. Absorption of hydrogen atoms from the metal surface into the lattice structure. For some metals, the increased concentration of surface hydrogen favors entrance of hydrogen atoms into the lattice structure of the metal.

$$\begin{array}{c} \overset{*}{M}\text{-}H \\ \downarrow \\ -M-M-M-M- \\ -M-M-M-M- \end{array} \rightarrow \begin{array}{c} \overset{*}{M} \\ \downarrow \\ -M-M-M-M- \\ -M-M-H-M-M- \end{array}$$

7. The removal of molecular hydrogen from the metal surface by one or more of the following possibilities:

(7a) Dissolution of molecular hydrogen into the solution at the metal-solution interface

$$\overset{*}{M}\text{-}H_{2_s} \rightarrow \overset{*}{M} + H_{2_{i,\text{dissolved}}}$$

(7b) Absorption of molecular hydrogen from the metal surface into the lattice structure of the metal

$$\begin{array}{c} \overset{*}{M}\text{-}H_2 \\ \downarrow \\ -M-M-M-M- \\ -M-M-M-M- \end{array} \rightarrow \begin{array}{c} \overset{*}{M} \\ \downarrow \\ -M-M-M-M- \\ -M-M-H_2-M-M- \end{array}$$

(7c) Formation of hydrogen gas bubbles on the metal surface and their subsequent detachment from the metal surface

$$n\ (\overset{*}{M}\text{-}H_2) \rightarrow M\text{-}(H_2)_n$$

where $M\text{-}(H_2)_n$ represents a hydrogen gas bubble attached on the metal surface:

$$M\text{-}(H_2)_n \rightarrow M + (H_2)_n$$

8. Desorption of metal ions from the metal surface

$$M_s^{++} \rightleftarrows M_i^{++}$$

9. Diffusion of the metal ions from the metal-solution interface to the bulk solution

$$M_i^{++} \rightarrow M_b^{++}$$

In aerated solutions, two other reactions can occur together with hydrogen evolution, namely, the oxygen depolarization and auto-catalytic reactions.

Investigators[15,16,28] have shown that the following successive stages are in good agreement with experimental data for the reaction of oxygen depolarization:

(i) Formation of a semivalent oxygen ion

$$O_2 + e \rightarrow O_2^-$$

(ii) Formation of perhydroxyl radical

$$O_2^- + H^+ \rightarrow HO_2$$

(iii) Formation of perhydroxyl ion

$$HO_2 + e \rightarrow HO_2^-$$

(iv) Formation of hydrogen peroxide

$$HO_2^- + H^+ \rightarrow H_2O_2$$

(v) Reduction of hydrogen peroxide with formation of hydroxyl ions

$$H_2O_2 + 2\,e \rightarrow 2\,OH^-$$

Many of these elementary stages are, today, no longer guesses but are experimentally proven facts. The detailed atomic mechanisms of this process may be represented by the following elementary stages:

10. Diffusion of oxygen from the bulk solution to the metal-solution interface

$$O_{2_b} \rightarrow O_{2_i}$$

where O_{2_b} denotes an oxygen molecule in the bulk solution, O_{2_i} denotes an oxygen molecule at the metal-solution interface;

11. Adsorption of oxygen on the active sites on the metal surface ; there are two types of adsorption possible for oxygen:

(11a) Molecular adsorption

$$\overset{*}{M} + O_{2_i} \rightleftarrows \overset{*}{M}\text{-}O_{2_s}$$

(11b) Dissociative adsorption

$$2\,\overset{*}{M} + O_{2_i} \rightleftarrows 2\,(\overset{*}{M}\text{-}O_s)$$

12. Formation of semivalent oxygen

(12a)

$$\text{- M - } \overset{\overset{*}{M}\text{-}O_2}{\overset{|}{M}} \text{ - M - M -} \rightarrow \text{- M - } \overset{\overset{*}{M}^{+}\text{-}O_2^{-}}{\overset{|}{M}} \text{ - M - M -}$$

(12b)

$$\text{- M - } \overset{\overset{*}{M}\text{-}O}{\overset{|}{M}} \text{ - } \overset{\overset{*}{M}\text{-}O}{\overset{|}{M}} \text{ - M - M -} \rightarrow \text{- M - } \overset{\overset{*}{M}^{+}\text{-}O^{-}}{\overset{|}{M}} \text{ - } \overset{\overset{*}{M}^{+}\text{-}O^{-}}{\overset{|}{M}} \text{ - M - M -}$$

13. Formation of perhydroxyl radical or hydroxyl radical

(13a) $$\overset{*}{M}^{+}\text{-}O_{2_s}^{-} + \overset{*}{M}\text{-}H_s^{+} \rightarrow \overset{*}{M}^{+}\text{-}HO_{2_s} + \overset{*}{M}_s$$

(13b) $$\overset{*}{M}^{+}\text{-}O_s^{-} + \overset{*}{M}\text{-}H_s^{+} \rightarrow \overset{*}{M}^{+}\text{-}HO_s + \overset{*}{M}_s$$

14. Formation of perhydroxyl ion by virtue of electron transfer

$$\overset{*}{M}^{+}\text{-}HO_{2_s} \rightarrow \overset{*}{M}^{++}\text{-}HO_{2_s}^{-}$$

15. Formation of hydrogen peroxide by one of the following possibilities:

(15a) $\underset{*}{M}^{++}\text{-}HO_{2_s}^{-} + \underset{*}{M}\text{-}H_s^{-} \rightarrow \underset{*}{M}\text{-}H_2O_{2_s} + \underset{*}{M}_s^{++}$

(15b) $2\,(\underset{*}{M}^{+}\text{-}HO) \rightarrow \underset{*}{M}\text{-}H_2O_{2_s} + \underset{*}{M}_s^{++}$

16. Reduction of hydrogen peroxide with the formation of hydroxyl ions: This step is itself a complex process and can be further broken down into the following sequence:

(16a) Reduction of hydrogen peroxide to hydroxyl ion and hydroxyl radical

$$\underset{*}{M}\text{-}H_2O_{2_s} \rightarrow \underset{*}{M}^{+}\text{-}HO_s + OH_i^{-}$$

(16b) Reduction of hydroxyl radical to hydroxyl ion

$$\underset{*}{M}^{+}\text{-}HO_s \rightarrow \underset{*}{M}_s^{++} + OH_i^{-}$$

17. Desorption of the metal ions from the metal surface

$$\underset{*}{M}_s^{++} \rightleftarrows M_i^{++}$$

18. Diffusion of the metal ions from the metal-solution interface to the bulk solution

$$M_i^{++} \rightarrow M_b^{++}$$

For metals that can exist in two or more oxidation states in acidic media, an autocatalytic reaction should be considered as a possibility. The following reaction scheme is suggested as a possible mechanism for this process when the ion of higher oxidation state is quadrivalent of the type M^{++++}:

19. An oxidation-reduction process in the bulk of the solution, at the metal-solution interface, or at the metal surface

(19a) $M_b^{++} + O_{2_b} + 2\,H_b^{+} \rightarrow M_b^{++++} + H_2O_{2_b}$

(19a) $\overset{*}{M}_i^{++} + O_{2_i} + 2\,H_i^{+} \rightarrow \overset{*}{M}_i^{++++} + H_2O_{2_i}$

(19b) $\overset{*}{M}_s^{++} + \overset{*}{M}\text{-}O_{2_s} + 2\,\overset{*}{M}\text{-}H_s^{+} \rightarrow \overset{*}{M}_s^{++++} + \overset{*}{M}\text{-}H_2O_{2_s} + 2\,\overset{*}{M}_s$

(19c) $\overset{*}{M}_s^{++} + \overset{*}{M}\text{-}O_s + \overset{*}{M}\text{-}H_s^{+} \rightarrow \overset{*}{M}_s^{++++} + \overset{*}{M}\text{-}OH_s^{-} + \overset{*}{M}$

20. An equilibrium between metal ions of higher and lower oxidation states by virtue of electron transfer, either at the metal surface or at the metal-solution interface.

(20a)

$$\begin{array}{ccc} -\overset{*}{M}^{++}- & -\overset{*}{M}^{++}-\overset{*}{M}- & -\overset{*}{M}^{++++}-\overset{*}{M}-\overset{*}{M}- \\ -M-\overset{|}{M}-M-\overset{|}{M}-\overset{|}{M}- & \rightleftarrows & -M-\overset{|}{M}-M-\overset{|}{M}-\overset{|}{M}- \end{array}$$

(20b) $M_i^{++++} + \overset{*}{M}_s \rightleftarrows 2\,M_i^{++}$

On the basis of the above discussion the following approach should be acceptable:

If it is not complicated by other factors, a typical corroding solution concentration-time plot for the dissolution of a metal capable of existing in two or more oxidation states in aerated solutions, will have the shape of curve C in Figure 3. It should be possible to divide the overall effect into three separate simultaneous corrosion processes. The proposed mechanisms of metal dissolution in acidic solutions, as represented by the elementary stages 1 to 18, suggest that the rates of hydrogen evolution and oxygen depolarization reactions are independent of the metal ion concentration in the solution (zero order dependency). Therefore, the corroding solution concentration-time plots for these two reactions should be straight lines as shown in Figure 3. In this diagram, the area under straight line A represent the dissolution effect

of hydrogen evolution. The area between straight lines A and B indicates the dissolution effect of oxygen depolarization. It should be noticed that the straight line B is asymptotic to the initial stage of curve C where the autocatalytic reaction is negligible. The region between curve C and straight line B represents the effect of the autocatalytic reaction.

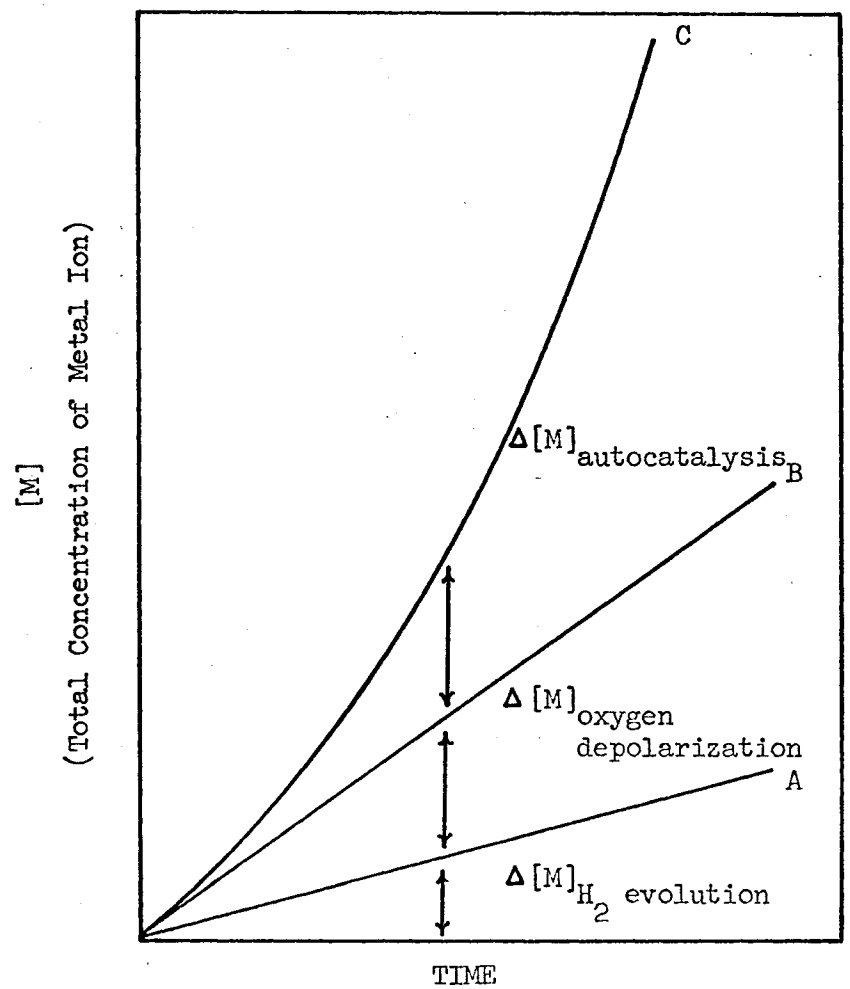

FIGURE 3. DISSOLUTION OF METAL IN ACIDIC MEDIA

CHAPTER V

EXPERIMENTAL RESULTS AND DISCUSSION

A. General Behavior of Tin Dissolution in Hydrochloric Acid Solutions

The analysis of the experimental data obtained in this study is based on the approach which was discussed previously in Chapter IV. A typical model of this analysis is illustrated in Figure 4 where curve A shows the rate data for the dissolution of tin in deareated (nitrogen gas saturated) hydrochloric acid solution, a condition under which only hydrogen evolution can occur. Curve C shows the rate data obtained under the same conditions as those of curve A except that the acid solution was air saturated.

Obviously, curve A conforms to a zero-order plot of metal ion concentration vs time. Here the exponential concentration-time plot of curve C is a confirmation of an autocatalytic process. Curve B is a straight line plotted asymptotically to curve C at its initial stage where autocatalysis is negligible. This is essentially an extension of the initial corrosion rate in the presence of oxygen. The total area under curve C is divided by straight lines A and B into three regions, each of which corresponds to a specific effect on the overall dissolution reaction as shown in Figure 4.

B. Rate Dependence on Tin Ion Concentration

As shown in Figure 5, the curved deviation from the linear zero-order initial rate plot, which is represented by the difference in metal ion concentration between curves B and C as shown in Figure 4, can

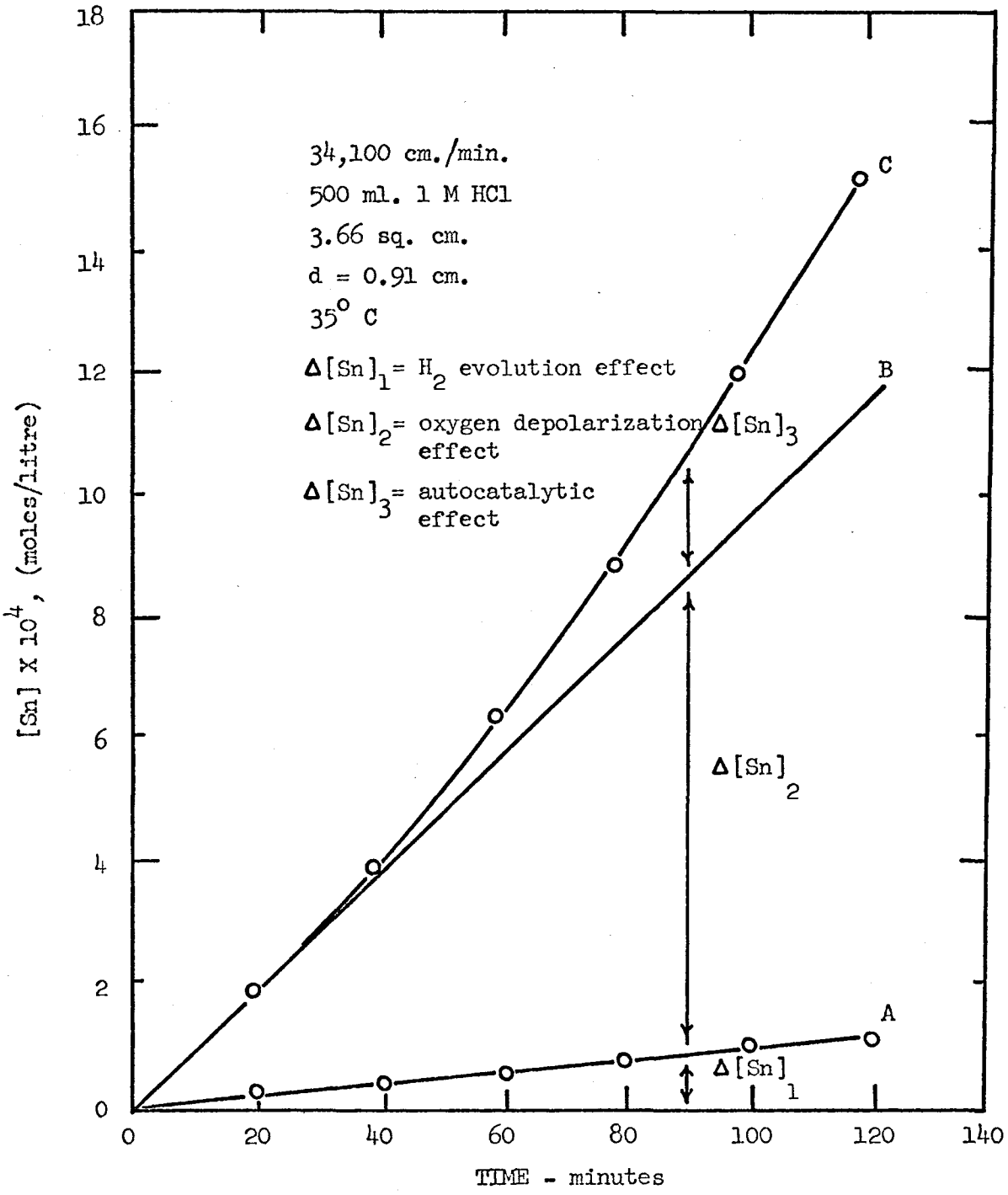

FIGURE 4. DISSOLUTION OF TIN IN HCl

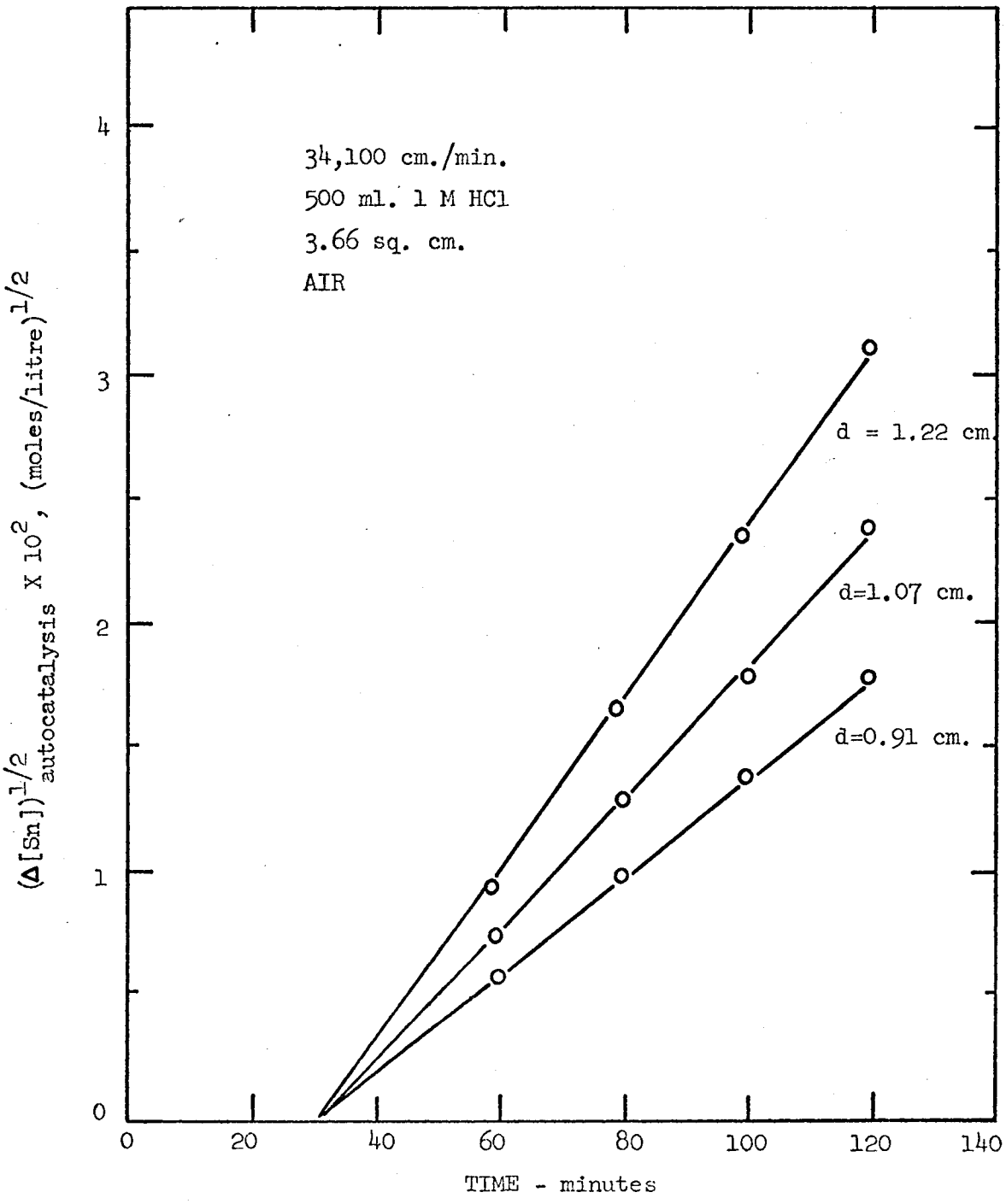

FIGURE 5. HALF-ORDER DEPENDENCE FOR AUTOCATALYTIC REACTION

be readily correlated by a half-order plot. All $(\Delta[Sn])^{1/2}$ vs time plots give straight lines. This is an indication that the autocatalytic process shows half-order dependence on metal concentration. From Figure 5, it can be observed that the autocatalytic reaction becomes important only after an elapsed time of 30 minutes.

C. Rate Dependence on Peripheral Velocity

The effect of peripheral velocity on the dissolution of tin was studied in both air- and nitrogen-saturated 1M HCl solutions for rotational speeds ranging from 1,000 to 12,000 rpm (2,840 - 34,100cm./min.). It was found that there is a considerable effect of peripheral velocity on tin dissolution.

Figures 6A and 6B illustrate that k_1, the rate constant for the hydrogen evolution reaction, and k_2, the oxygen depolarization reaction rate constant are both proportional to peripheral velocity raised to the 0.98 power. The effect of peripheral velocity on k_3, the rate constant for the autocatalytic process, as shown in Figure 7, can be represented by an equation of the form:

$$k_3 = k_3' [v]^n$$

where: $n = 0.30$ for $2,840 < v < 21,230$ cm./min.

$n = 0.90$ for $21,230 < v < 34,100$ cm./min.

It is not apparent why the velocity effect shows two distinct regions for the rate constant of the autocatalytic process. Lui[24] reported a somewhat similar behavior which he related to hydrogen bubble formation at varies speeds:

"Tin evolves hydrogen gas from hydrochloric acid, but it was impossible to detect any gas bubble on the metal surface in 1M HCl. By

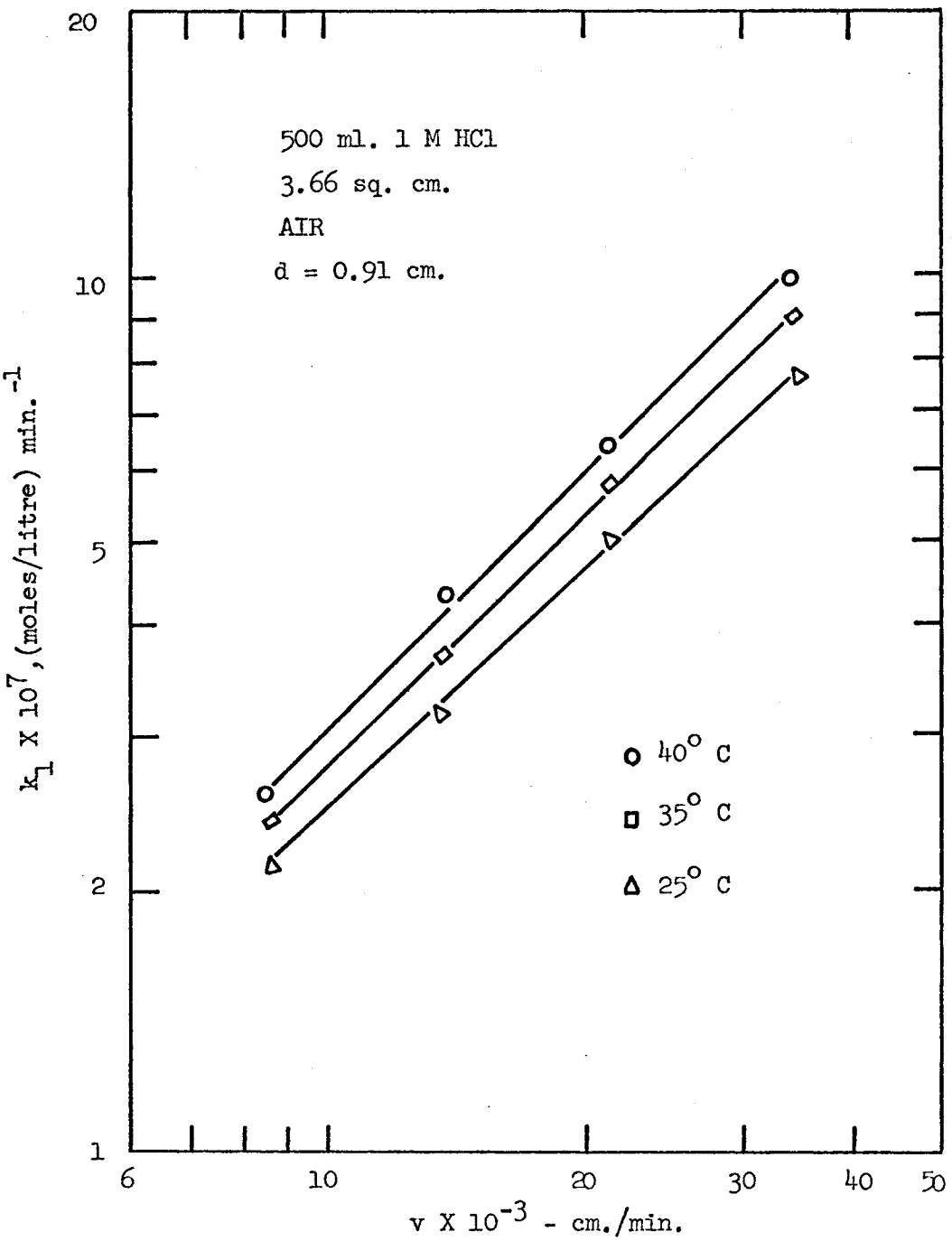

FIGURE 6A. DISSOLUTION AS FUNCTION OF PERIPHERAL VELOCITY

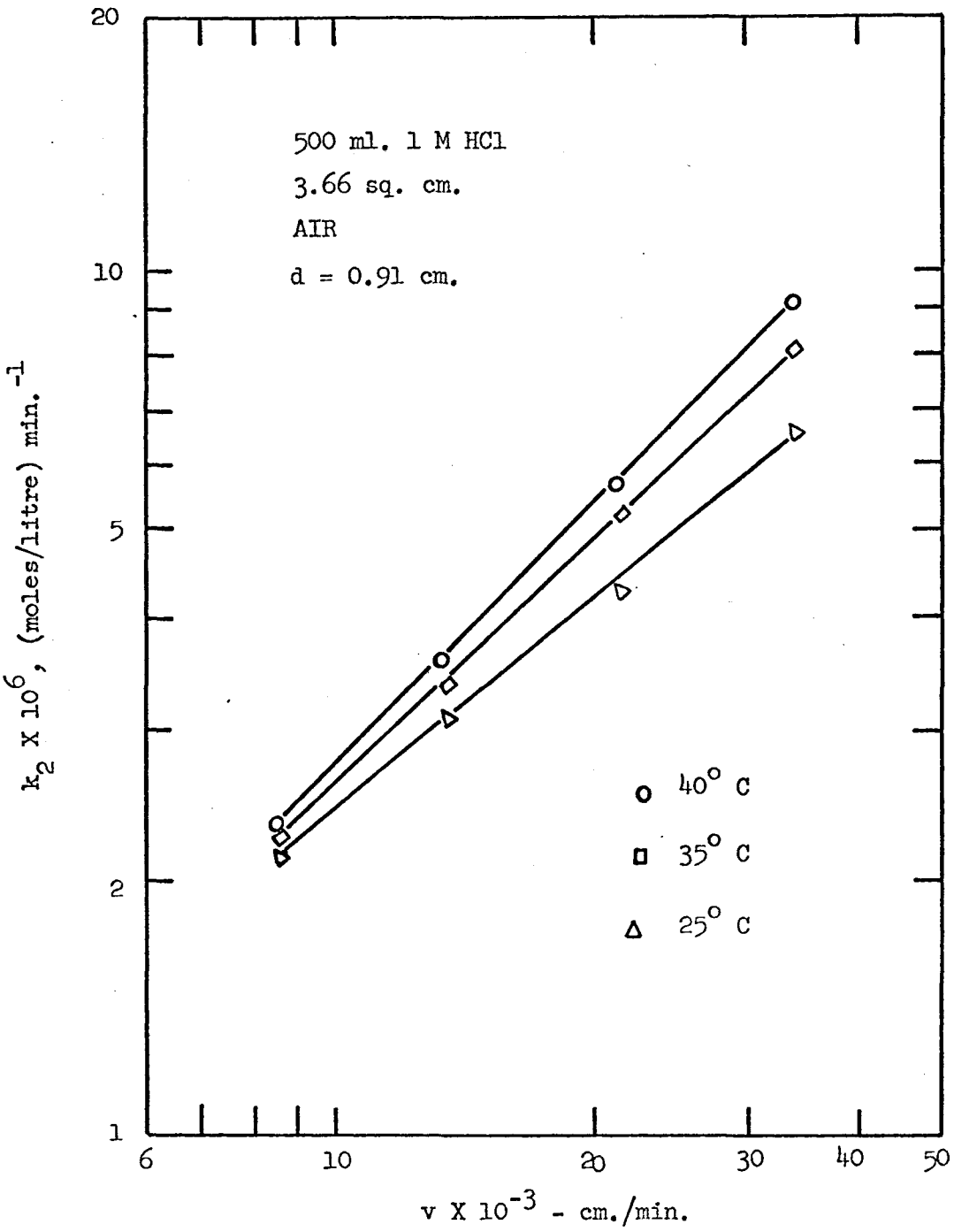

FIGURE 6B. DISSOLUTION AS FUNCTION OF PERIPHERAL VELOCITY

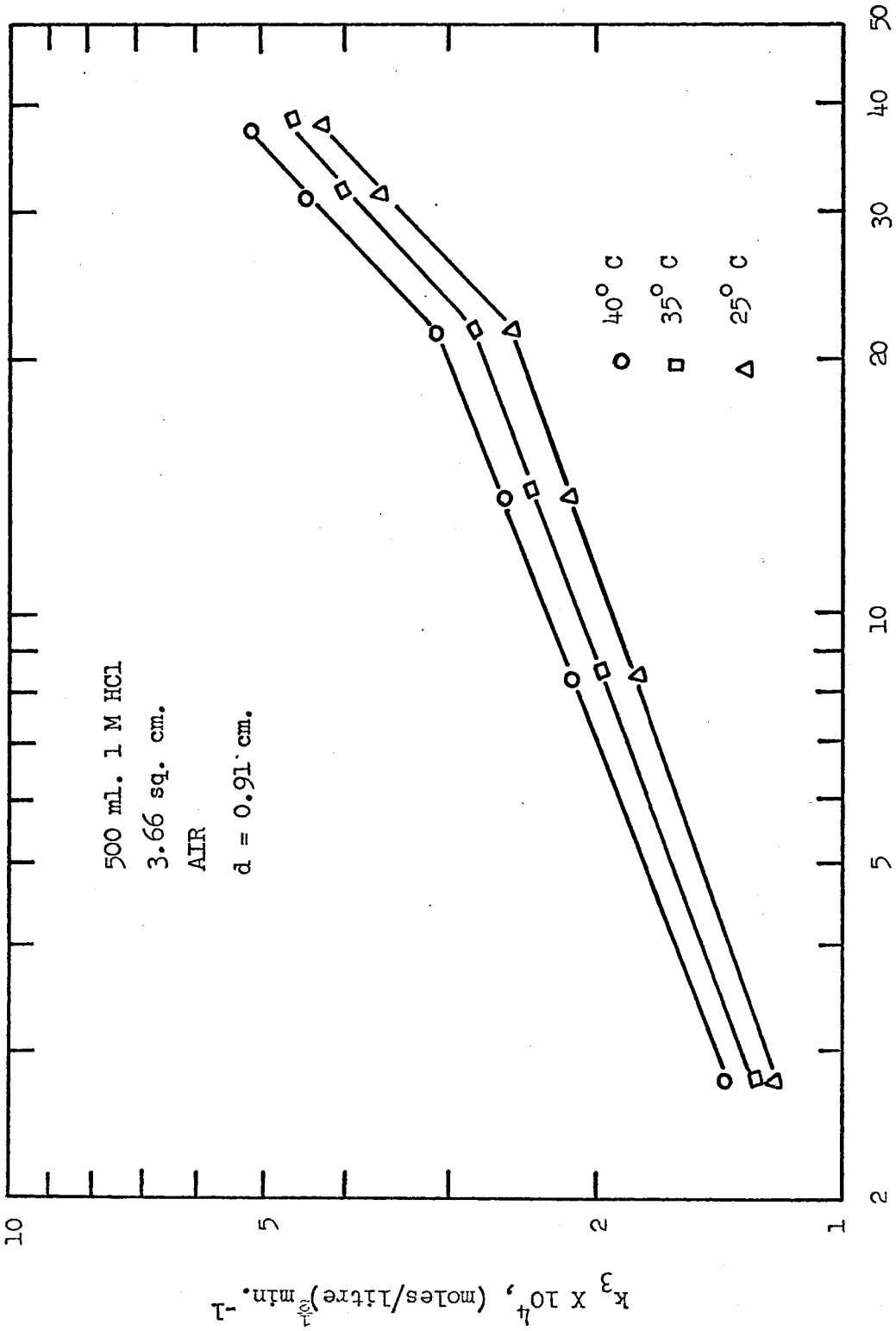

FIGURE 7. DISSOLUTION AS FUNCTION OF PERIPHERAL VELOCITY

corroding specimens in 6M HCl it was easy to observe gas bubble formation. Rotation of the sample at speeds below 3,000 rpm did not remove all of the large bubbles. Over the range 3,000 to 11,000 rpm, the large visible bubbles were removed from the surface quite readily but very small ones were still attached to the metal surface. Above 11,000 rpm no bubbles were observed on the metal surface.

Although such behavior cannot be observed in 1M HCl solutions, it is not unreasonable to expect some comparable elimination of hydrogen bubbles from corroding surfaces. At low velocity, the corroding surface is protected by the hydrogen gas bubbles."[24]

In the present work no studies were done on hydrogen bubble formation.

D. Rate Dependence on Temperature

The rate constant dependence on temperature was studied over the range 25 to 45°C under nitrogen, air, and oxygen saturation. The results are illustrated by the Arrhenius' activation energy plots shown in Figures 8 to 10.

The temperature variations correspond to apparent activation energies of 3.06 kcal per mole for the hydrogen evolution reaction and 3.66 kcal per mole for the oxygen depolarization. These low values suggest that both reactions are under complete diffusional control[1,13]. The activation energy for the autocatalytic process is of the order of 5.54 kcal per mole, a value somewhat larger than the 3-4 kcal per mole to be expected for a simple diffusion process.

The activation energies for the autocatalytic process, as illustrated in Figure 11, were essentially constant for varying sample

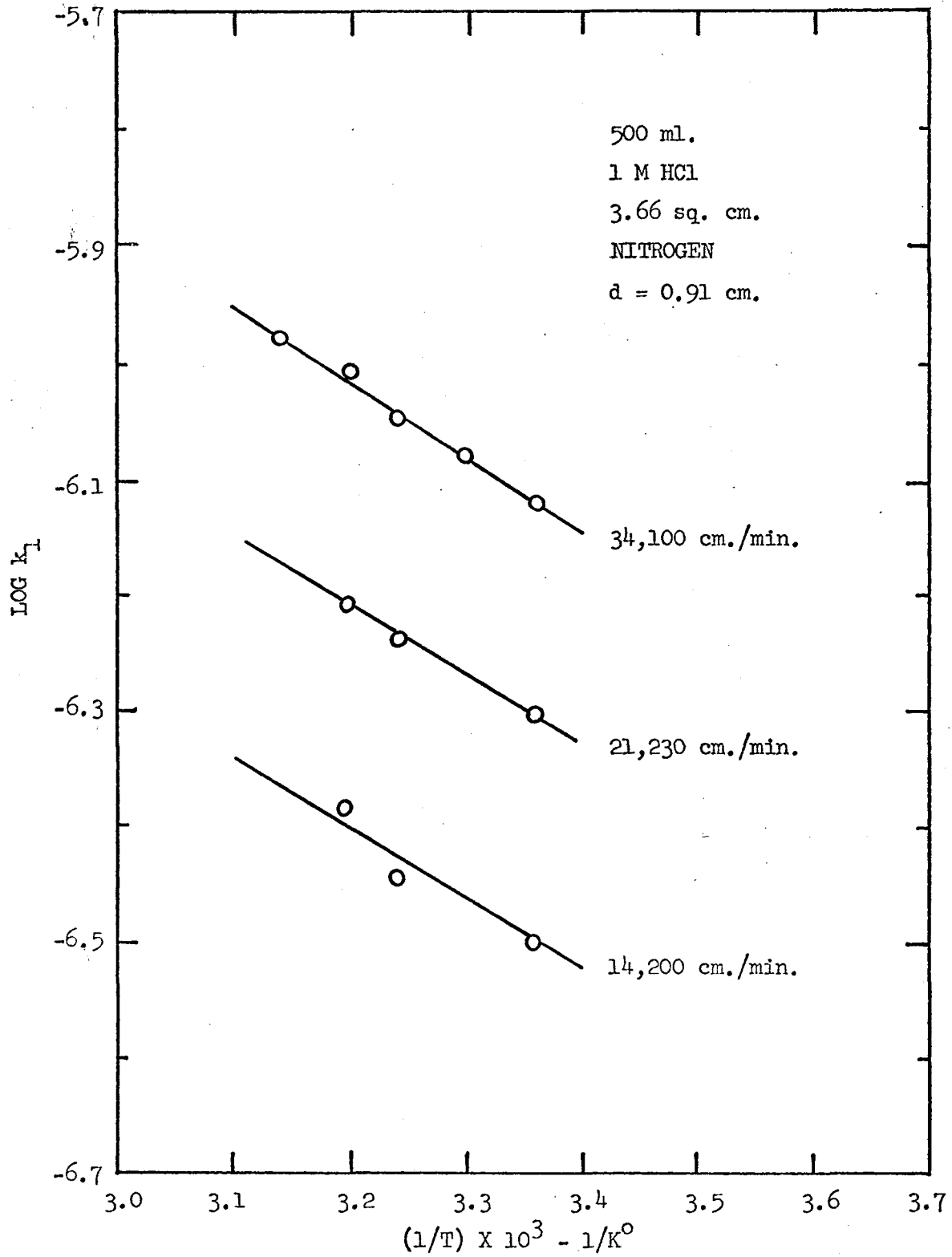

FIGURE 8. DISSOLUTION AS FUNCTION OF TEMPERATURE

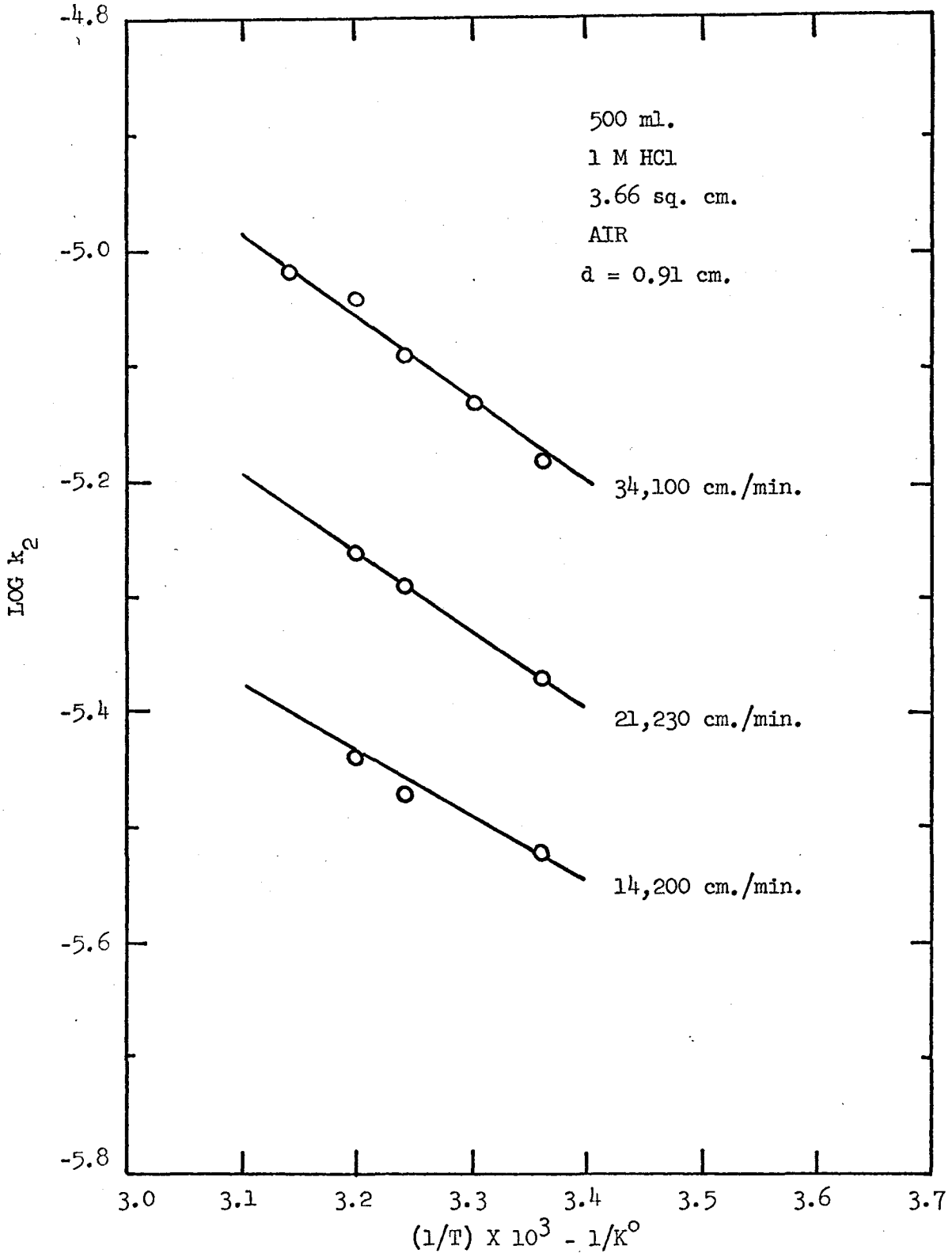

FIGURE 9. DISSOLUTION AS FUNCTION OF TEMPERATURE

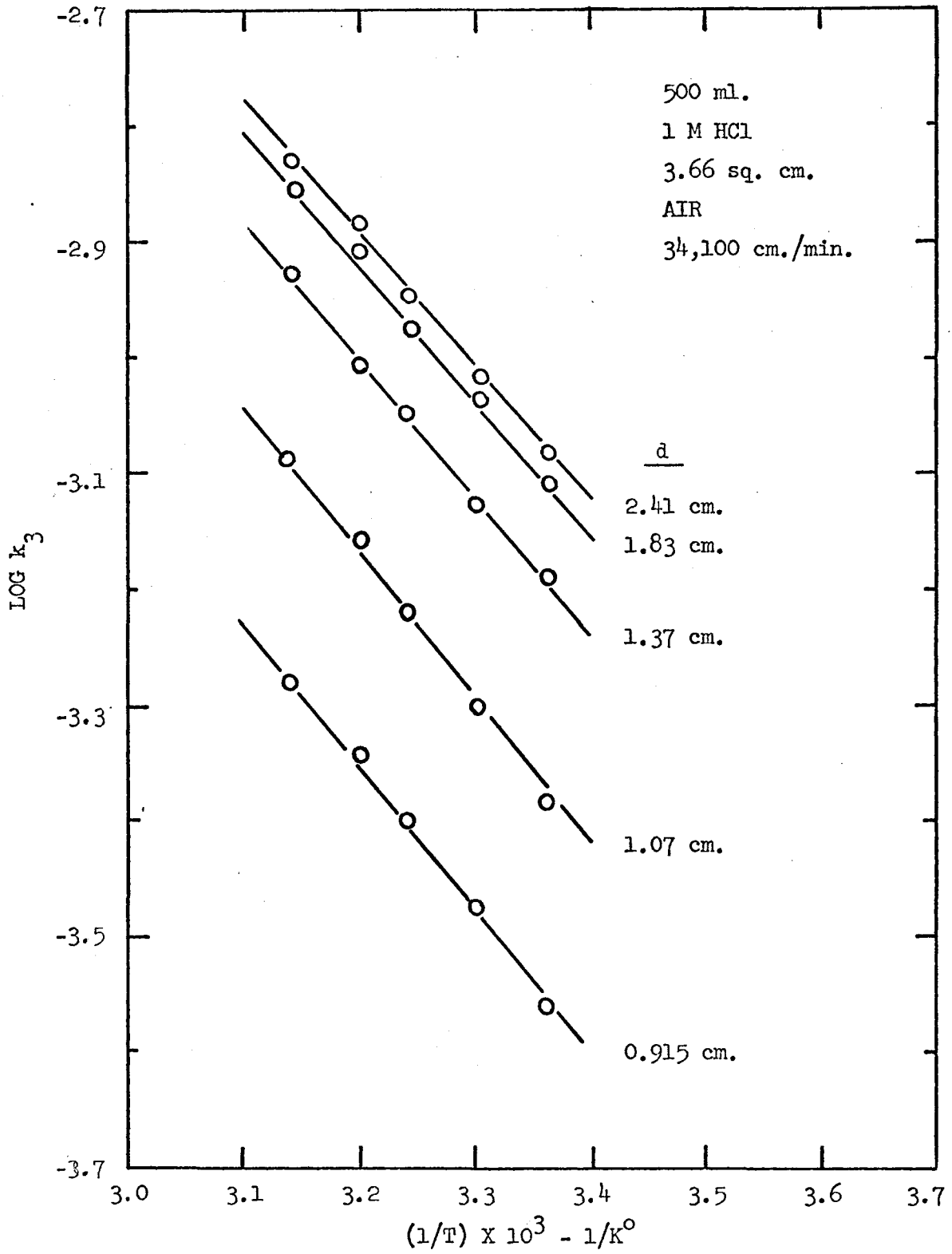

FIGURE 10. DISSOLUTION AS FUNCTION OF TEMPERATURE

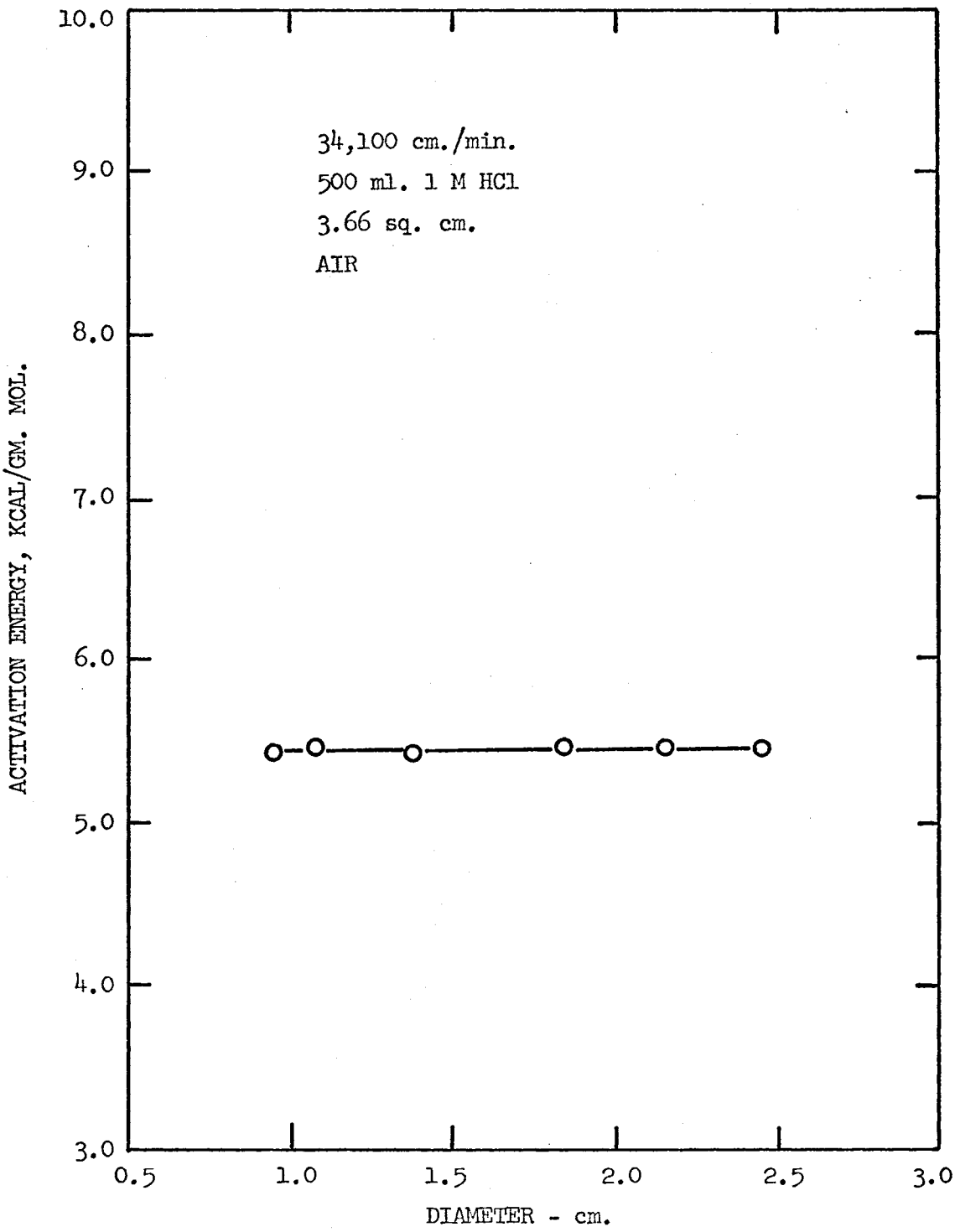

FIGURE 11. ACTIVATION ENERGY AS FUNCTION OF SAMPLE DIAMETER (autocatalytic reaction)

diameters and rotational speeds corresponding to constant peripheral velocity.

E. Rate Dependence on Sample Surface Area and Corroding Solution Volume

The effect of varying the solution volume and sample surface area was investigated by Lui[24] at 30°C in air saturated 1M HCl solutions. A re-examination of his data shows that for changes in the surface area from 0.91 to 7.32 $cm.^2$, and in solution volume from 400 to 600 ml the rate constants k_1 and k_2 are directly proportional to A/V, as shown in Figures 12 and 13.

Figures 14 and 15 illustrate that the rate constant for the autocatalytic reaction, k_3, is proportional to $[A]^{1/2}/V$ ratio.

F. Effect of Hydrochloric Acid Concentration

The effect of hydrochloric acid concentration was studied by Lui[24] who rotated the samples in aerated and deaerated solutions over the concentration range 0.10 to 4.10 M HCl. Analysis of his data according to the scheme suggested in this project also shows that the dissolution rate of tin is essentially independent of acid concentration. Table 1 indicates that there is no apparent trend for k_1 and k_3 over the range of concentration studied. Since the quantity $(k_1 + k_2)$ appears to be also independent of acid concentration, this means that k_2 alone is independent of acid concentration.

Dissolution rates independent of acid concentration were reported by other investigators[6,23]. At present there are no valid explanations for this behavior.

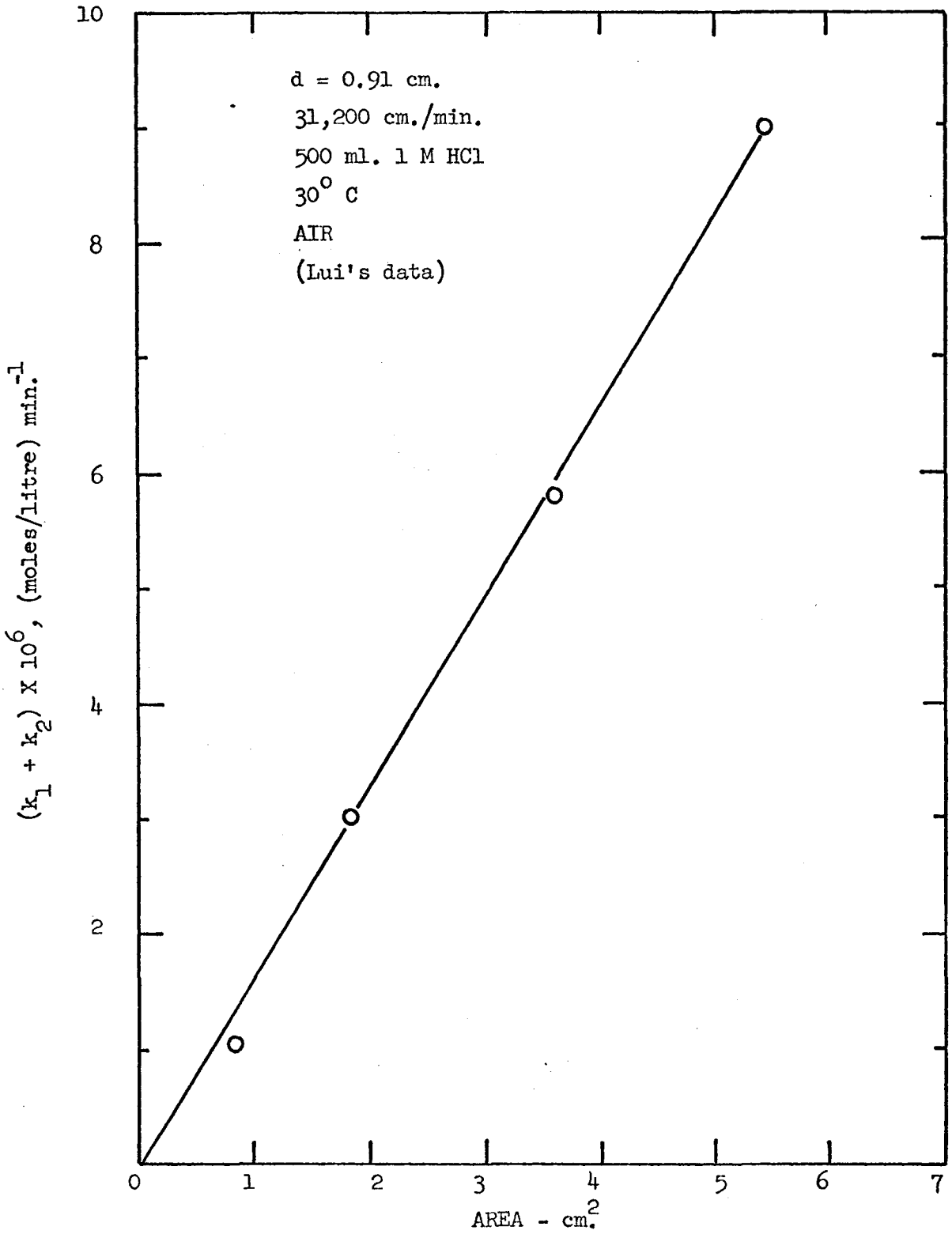

FIGURE 12. DISSOLUTION AS FUNCTION OF SURFACE AREA

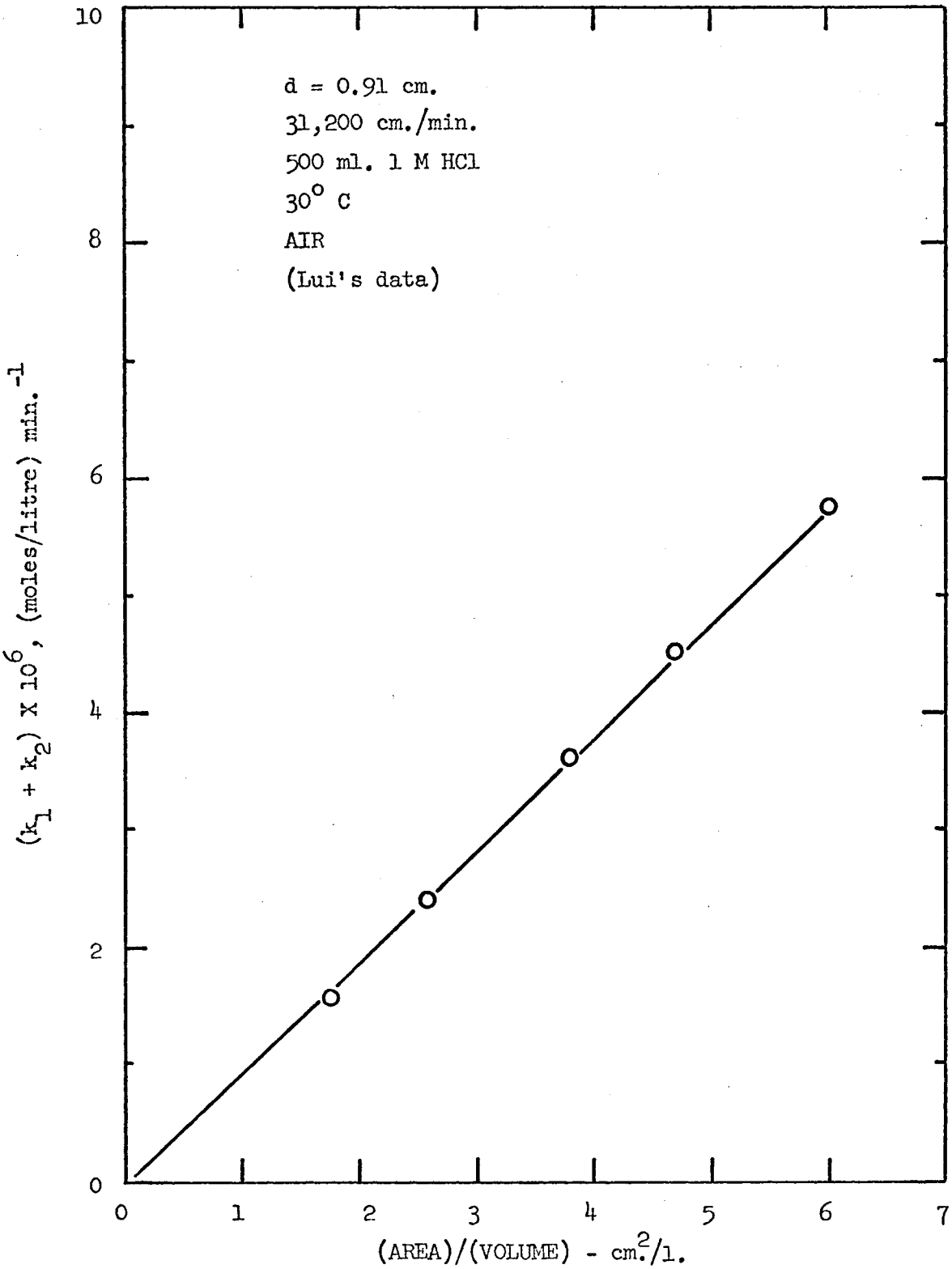

FIGURE 13. DISSOLUTION AS FUNCTION OF A/V

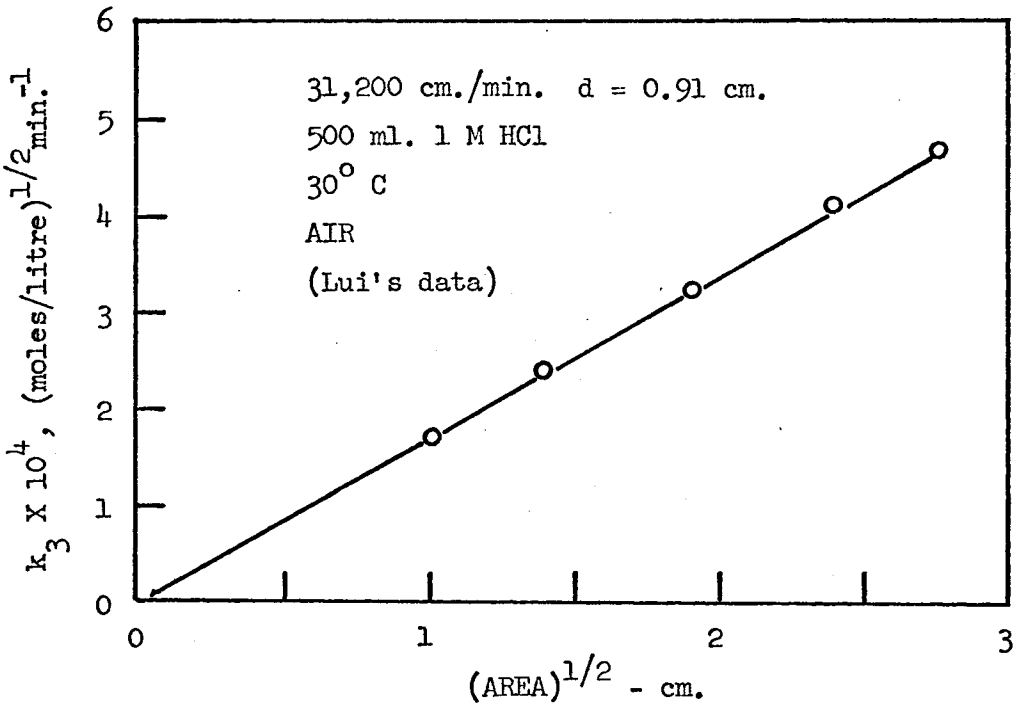

FIGURE 14. DISSOLUTION AS FUNCTION OF AREA

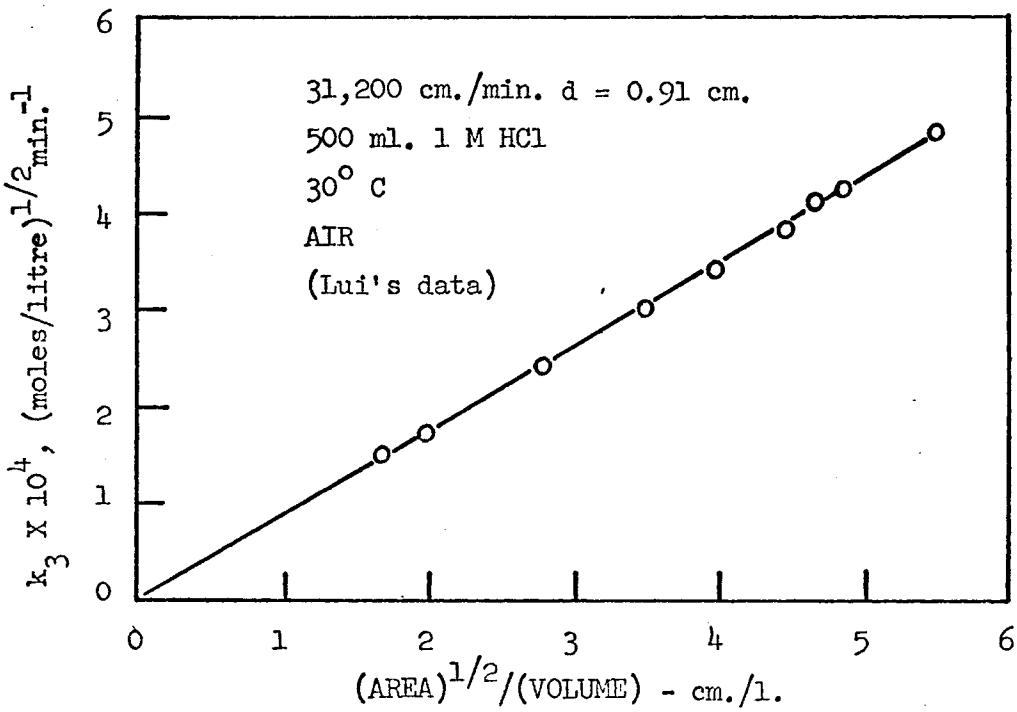

FIGURE 15. DISSOLUTION AS FUNCTION OF A/V

TABLE 1

Effect of Hydrochloric Acid Concentration on Dissolution Rates

[HCl] (M)	k_1 (mol./l.min.)	$k_1 + k_2$ (mol./l.min.)	k_3 $(mol./l.)^{1/2} min.^{-1}$
0.101		7.0×10^{-6}	2.5×10^{-5}
0.146		9.1	3.2
0.323		6.5	3.0
0.401		7.0	2.9
0.495	7.5×10^{-7}		
0.546		7.6	3.0
0.802		6.4	2.6
1.000		7.0	3.1
1.004	8.0		
2.050		6.8	2.4
2.120	8.0		
2.800	7.9		
2.875		6.6	3.3
4.030		6.6	3.4

G. Rate Dependence on Oxygen Concentration

The influence of oxygen concentration on the dissolution rate of tin was determined by investigating, respectively, the reaction rates in nitrogen, air, and oxygen saturated acid solutions. Figure 16 shows that the rate of dissolution is well correlated in terms of the square root of the oxygen partial pressure in the gas phase with which the solution is equilibrated. The rate constants k_2 and k_3 are directly proportional to the square root of the oxygen partial pressure.

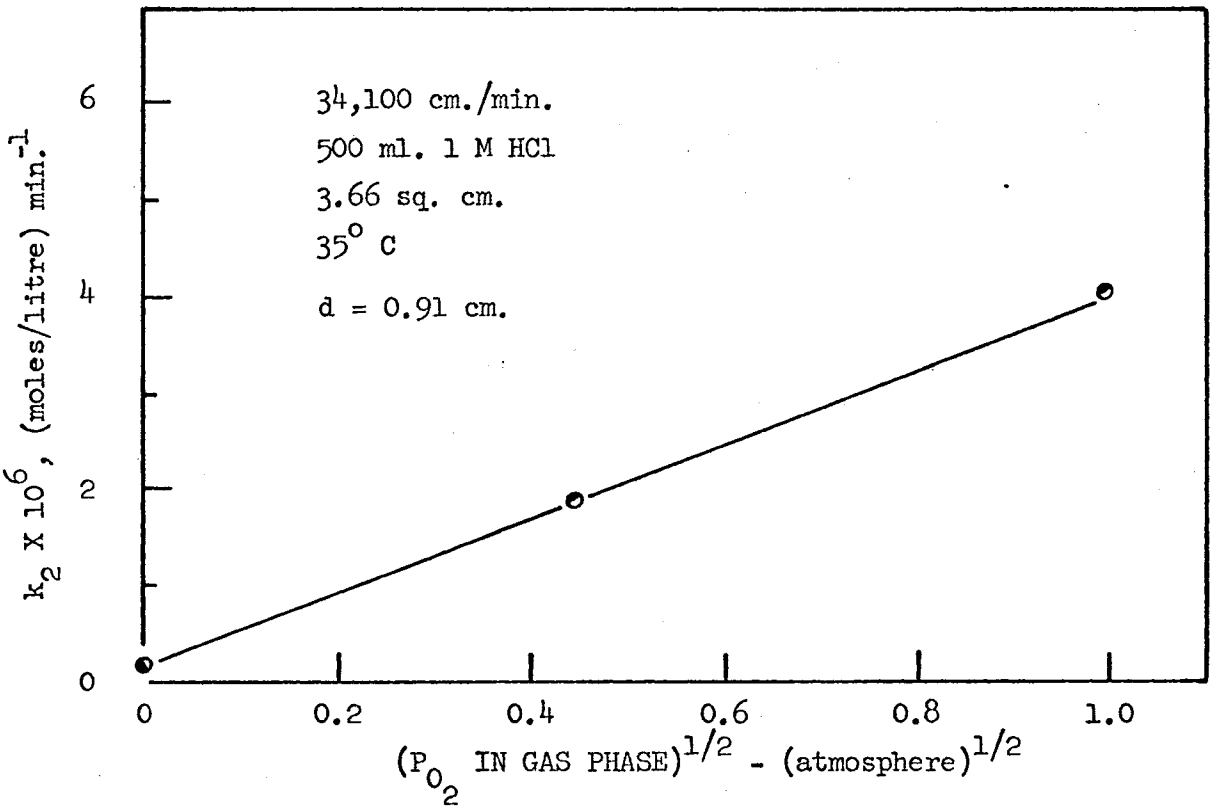

FIGURE 16A. EFFECT OF OXYGEN CONCENTRATION

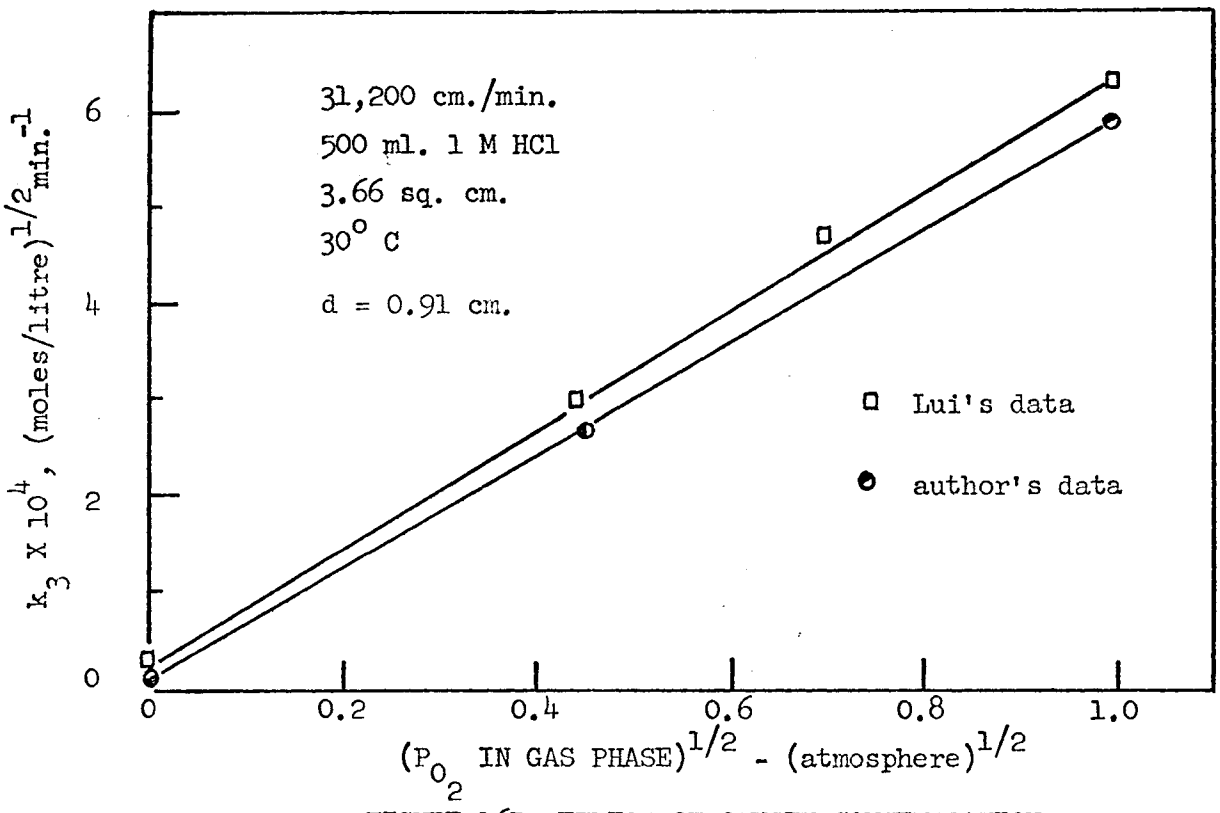

FIGURE 16B. EFFECT OF OXYGEN CONCENTRATION

H. The Effect of Hydrodynamic Factors

The effect of flow pattern on dissolution rate was studied at 35^{o} C in aerated 1M HCl solutions. The variation of flow pattern near the metal surface was effected by changing the sample diameter. This change of diameter was accompanied by a proportional change in rpm and sample length to keep the peripheral velocity and surface area at constant values of 34,100 cm./min. and 3.66 $cm.^{2}$, respectively.

The Plexiglas protected, rotating shaft used in this study was 0.915 cm. in diameter, therefore, when a sample of the same diameter was fitted onto the shaft a uniform surface was formed and no turbulence near the sample surface could be observed when samples of this type were rotated in the corroding solution. However, when the sample diameter increased, its surface stood out from the shaft. Strong turbulence around the sample caused by this non-uniformity of surface could be easily observed when samples of larger diameter were rotated in solution.

The results of this investigation, as presented in Figures 17 to 19, point out that all three rate constants, k_1, k_2, and k_3 increased with increasing sample diameter for the range 0.915 to 1.52 cm., but further increase in diameter has no effect on the dissolution rate.

This behavior may be interpreted by the equation of diffusional mass flux given by Levich[17] as

$$J = (D + D_{turb}) \frac{\partial c}{\partial y}$$

$$= (D + \beta \overline{l v}) \frac{\partial c}{\partial y}$$

The dissolution increases initially as l, the average value of eddy scale of turbulence, and $\frac{\partial c}{\partial y}$ increase to maximum values determined

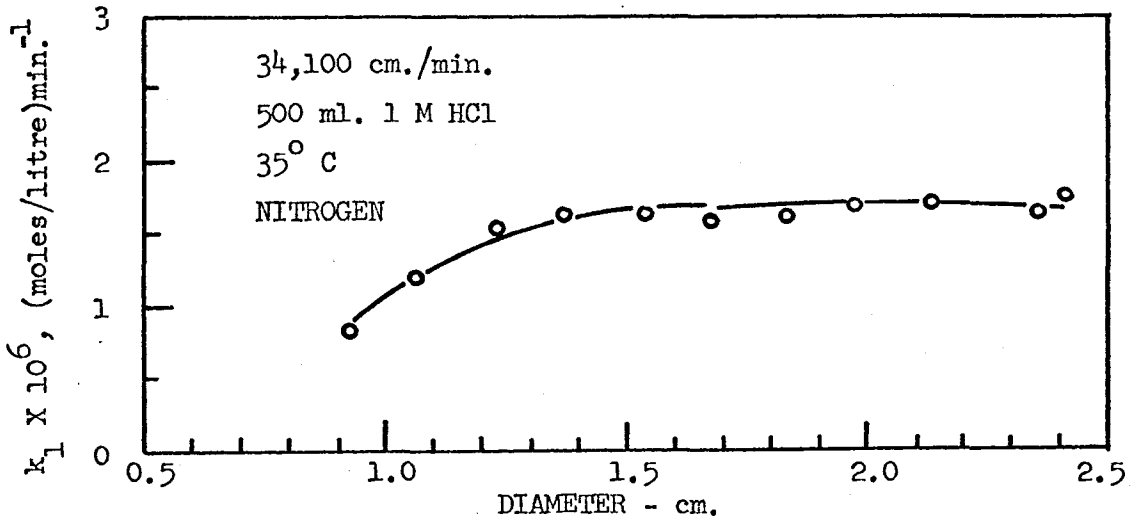

FIGURE 17. EFFECT OF HYDRODYNAMIC FACTORS

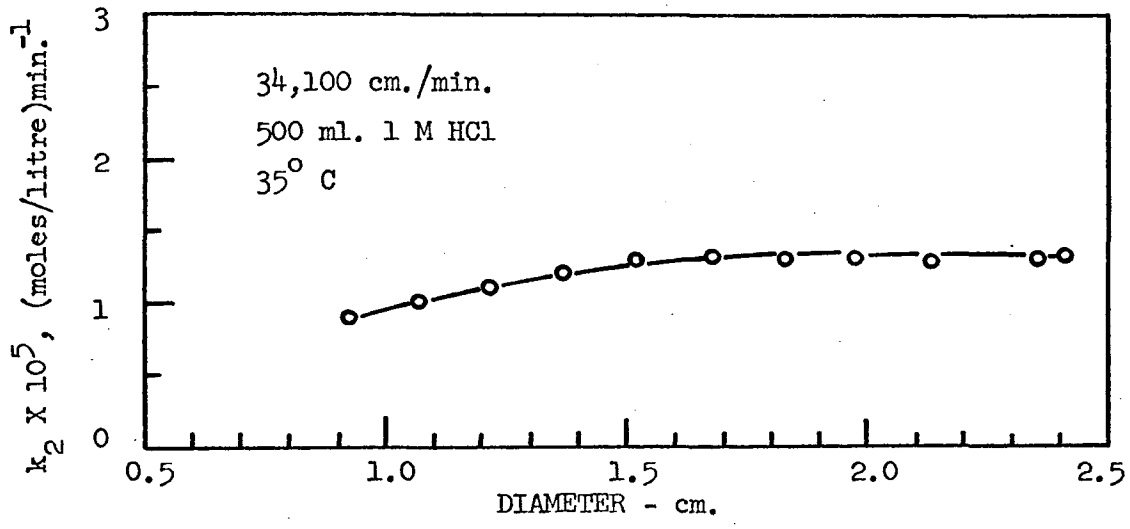

FIGURE 18. EFFECT OF HYDRODYNAMIC FACTORS

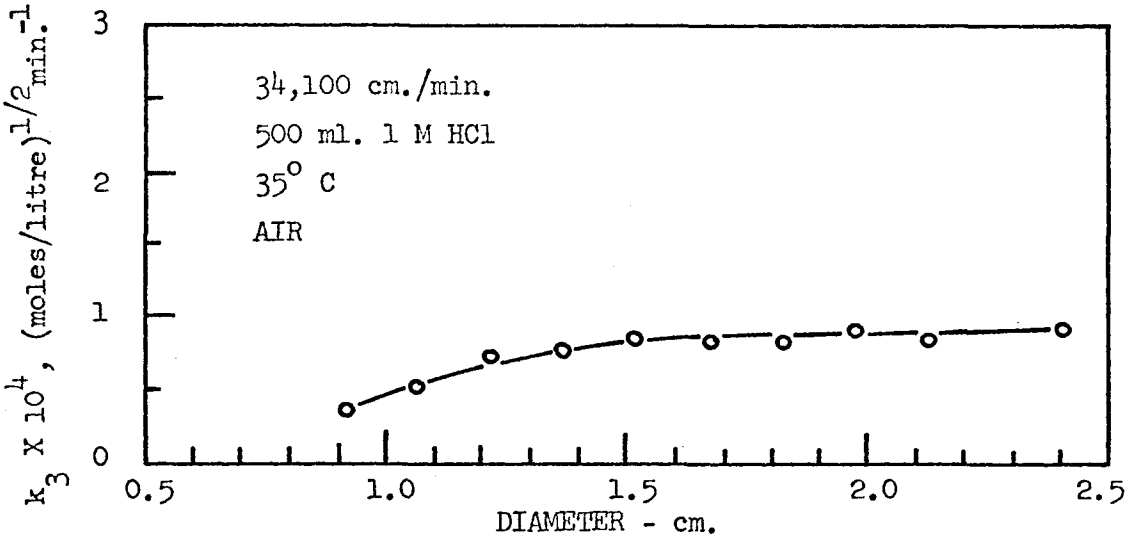

FIGURE 19. EFFECT OF HYDRODYNAMIC FACTORS

by the geometry of the system. In general the change in $\frac{\partial c}{\partial y}$ should be negligible because the peripheral velocity of the sample was kept constant.

A more important factor may be the accumulation of hydrogen gas on the corroding surface. Metals that displace hydrogen from acidic media show peculiar rate vs area relationships when area changes are accomplished by increasing the height of constant diameter cylindrical specimens. It is suspected that the upward movement of hydrogen gas bubbles may offer some protection to the corroding surface at it upper regions. With very short samples the increased diameter becomes responsible for some turbulent flow patterns that may be effective in sweeping the surface clean of attached gas bubbles. More work is required before this phenomenon may be appreciated completely.

I. Mechanism of Tin Dissolution in Hydrochloric Acid

On the basis of the established experimental results, tin dissolution may be interpreted in terms of the following mechanism:

1. The reaction scheme proposed for the hydrogen evolution reaction is:

(1a) Diffusion of hydrogen ions from the bulk solution to the metal-solution interface

$$H_b^+ \rightarrow H_i^+$$

(1b) Adsorption of hydrogen ions on metal surface

$$H_i^+ + \underset{*}{Sn} \rightleftarrows \underset{*}{Sn}\text{-}H_s^+$$

(1c) Formation of atomic hydrogen

$$\underset{*}{Sn}\text{-}H_s^+ \rightarrow \underset{*}{Sn^+}\text{-}H_s$$

(1d) Formation of molecular hydrogen from atomic hydrogen

$$2\ \underset{*}{Sn^+}\text{-}H_s \rightarrow \underset{*}{Sn}\text{-}H_{2_s} + \underset{*}{Sn_s^{++}}$$

(1e) Removal of hydrogen molecules from the metal surface, either by dissolution into the solution or by the formation of gas bubbles and their subsequent detachment from the metal surface

$$\overset{*}{Sn}\text{-}H_{2_s} \rightarrow \overset{*}{Sn}_s + H_{2_{i,dissolved}}$$

$$n\,(\overset{*}{Sn}\text{-}H_{2_s}) \rightarrow n\,\overset{*}{Sn} + n\,H_2$$

where nH_2 denotes a hydrogen gas bubble

(1f) Desorption of stannous ions from the metal surface to the metal-solution interface

$$\overset{*}{Sn}^{++}_s \rightleftarrows Sn^{++}_i$$

(1g) Diffusion of stannous ions from the metal-solution interface to the bulk solution

$$Sn^{++}_i \rightarrow Sn^{++}_b$$

2. In aerated hydrochloric acid solution, the tin dissolution is accelerated by two other simultaneous reactions. These are oxygen depolarization and autocatalysis.

The mechanism proposed for the oxygen depolarization can be described by the following elementary stages:

(2a) Diffusion of oxygen from the bulk solution to the metal-solution interface

$$O_{2_b} \rightarrow O_{2_i}$$

(2b) Adsorption of oxygen on the metal surface

$$O_{2_i} + 2\,\overset{*}{Sn} \rightleftarrows 2\,(\overset{*}{Sn}\text{-}O_s)$$

(2c) Formation of oxygen ion by virtue of electron transfer

$$\overset{*}{Sn}\text{-}O_s \rightarrow \overset{*}{Sn}^{+}\text{-}O_s^{-}$$

(2d) Formation of hydroxyl radical

$$\overset{*}{Sn}^{+}\text{-}O_s^{-} + \overset{*}{Sn}\text{-}H_s^{+} \rightarrow \overset{*}{Sn}^{+}\text{-}HO_s + \overset{*}{Sn}_s$$

(2d) Formation of hydrogen peroxide

$$2\,(\overset{*}{Sn}^{+}\text{-}OH) \rightarrow \overset{*}{Sn}\text{-}H_2O_{2_s} + \overset{*}{Sn}_s^{++}$$

(2f) Reduction of hydrogen peroxide with formation of hydroxyl ions

$$\overset{*}{Sn}\text{-}H_2O_{2_s} \rightarrow \overset{*}{Sn}^{+}\text{-}HO_s + OH^{-}$$

$$\overset{*}{Sn}^{+}\text{-}HO_s \rightarrow \overset{*}{Sn}_s^{++} + OH^{-}$$

(2g) Desorption of stannous ions from the metal surface to the metal-solution interface

$$\overset{*}{Sn}_s^{++} \rightleftarrows Sn_i^{++}$$

(2h) Diffusion of stannous ions from the metal-solution interface to the bulk solution

$$Sn_i^{++} \rightarrow Sn_b^{++}$$

3. The following reaction scheme is proposed for the autocatalytic reaction:

(3a) An oxidation-reduction process occurred at the metal surface

$$\overset{*}{Sn}_s^{++} + \overset{*}{Sn}^{+}\text{-}O_s^{-} + \overset{*}{Sn}\text{-}H_s^{+} \rightarrow \overset{*}{Sn}_s^{++++} + \overset{*}{Sn}\text{-}OH_s^{-} + \overset{*}{Sn}_s$$

(3b) The stannous, stannic species equilibrium is established at all times at the metal surface

$$\overset{*}{Sn}_s + \overset{*}{Sn}_s^{++++} \rightleftarrows 2\,\overset{*}{Sn}_s^{++}$$

As reported by other investigators[24,25], the specimen surface became coated with a gray film during tin dissolution in acidic media. Chemical analysis[25] and X-ray diffraction analysis[24] of the surface film showed that it consisted of redeposited pure tin.

J. Empirical Rate Equation for Tin Dissolution

The experimental data discussed above for the dissolution of tin in hydrochloric acid solutions in the presence or absence of oxygen may be summarized by the equation:

$$\frac{d}{dt}[Sn] = k_1^o \frac{A}{V}[HCl]^0[v]^{0.98} e^{-\frac{3060}{RT}} + k_2^o \frac{A}{V}[HCl]^0[v]^{0.98}[P_{O_2}]^{1/2} e^{-\frac{3660}{RT}} + k_3^o \frac{[A]^{1/2}}{V}[HCl]^0[v]^n[P_{O_2}]^{1/2}[Sn]^{1/2} e^{-\frac{5440}{RT}}$$

where: $n = 0.30$ for $2{,}840 < v < 21{,}230$ cm./min.

$n = 0.90$ for $21{,}230 < v < 34{,}100$ cm./min.

Range of experimental conditions:

$T = 298 - 318^o$ K

$A = 0.91 - 7.32$ sq.cm.

$V = 400 - 600$ ml

$P_{O_2} = 0 - 1.0$ atm.

$v = 2{,}840 - 34{,}100$ cm./min.

$[HCl] = 0.10 - 4.03$ M

$d = 0.915$ cm.

The following equations:

$$k_1^o = \frac{V}{A} \frac{1}{[v]^{0.98}} e^{\frac{3060}{RT}} \frac{d[Sn]}{dt} \quad (H_2 \text{ evolution})$$

$$k_2^o = \frac{V}{A} \frac{1}{[v]^{0.98}} \frac{1}{[P_{O_2}]^{1/2}} e^{\frac{3660}{RT}} \frac{d[Sn]}{dt} \quad (O_2 \text{ depolarization})$$

$$k_3^o = 2 \frac{V}{[A]^{1/2}} \frac{1}{[v]^n} \frac{1}{[P_{O_2}]^{1/2}} e^{\frac{5440}{RT}} \frac{d[Sn]^{1/2}}{dt} \quad (\text{autocatalysis})$$

have been used for the determination of k_1^o, k_2^o, and k_3^o to give the average values of these constants, with an average deviation of $\pm$ 4 per cent as shown in Tables 2, 3, and 4.

TABLE II

EVALUATION OF VELOCITY CONSTANT
(k_1^o for hydrogen evolution)

$\frac{d[Sn]}{dt}$ (mol./l.min.)	T (°C)	A ($cm.^2$)	V (ml)	v (cm./min.)	k_1^o
0.756×10^{-6}	25	3.66	500	34,100	5.28×10^{-7}
0.830	30				5.30
0.907	35				5.37
0.980	40				5.31
1.050	45				5.30
0.208	30	0.91		31,600	5.33
0.413		1.83			5.26
0.828		3.66			5.27
1.290		5.49			5.34
					5.31 average

TABLE III
EVALUATION OF VELOCITY CONSTANT
(k_2^o for oxygen depolarization)

$\frac{d[Sn]}{dt}$ (mol./l.min.)	T (°C)	A ($cm.^2$)	V (ml.)	v (cm./min.)	P_{O_2} (atm.)	k_2^o
0.55×10^{-5}	25	3.66	500	34,100	0.21	2.28×10^{-5}
0.62	30					2.33
0.67	35					2.25
0.70	40					2.20
0.80	45					2.28
0.13	30	0.91				2.11
0.28		1.83				2.26
0.57		3.66				2.36
0.88		5.49				2.41
						2.28 average

TABLE IV
EVALUATION OF VELOCITY CONSTANT
(k_3^o for autocatalytic reaction)

$\frac{d[Sn]^{1/2}}{dt}$ $(mol./l.)^{1/2}min.^{-1}$	T (°C)	A ($cm.^2$)	V (ml.)	v (cm./min.)	P_{O_2} (atm.)	k_3^o
2.72×10^{-4}	25	3.66	500	34,100	0.21	1.20×10^{-1}
3.35	30					1.27
4.00	35					1.32
4.50	40					1.26
5.20	45					1.29
1.55	30	0.91		31,600		1.20
2.24		1.83				1.23
3.00		3.66				1.27
3.65		5.49				1.16
						1.25 average

Therefore, the empirical rate equation for the dissolution of tin becomes:

$$\frac{d}{dt}[Sn] = 5.31 \times 10^{-7} \frac{A}{V} [HCl]^{0}[v]^{0.98} e^{-\frac{3060}{RT}}$$

$$+ \quad 2.88 \times 10^{-5} \frac{A}{V} [HCl]^{0}[v]^{0.98}[P_{O_2}]^{1/2} e^{-\frac{3660}{RT}}$$

$$+ \quad 1.25 \times 10^{-1} \frac{[A]^{1/2}}{V} [HCl]^{0}[v]^{n}[P_{O_2}]^{1/2}[Sn]^{1/2} e^{-\frac{5440}{RT}}$$

in which the third term (autocatalytic) applies only after an elapsed time of 30 minutes.

CHAPTER VI

CONCLUSIONS

1. The tin dissolution reaction appears to occur through parallel reaction paths. In deaerated acid solutions there is a slow reaction due to a simple hydrogen evolution process. In aerated acid solutions there are three simultaneous reactions, hydrogen evolution, oxygen depolarization, and an autocatalytic process. The last reaction is important only after a short initial period.

2. On the basis of the established experimental results, it is reasonable to conclude that the hydrogen evolution and oxygen depolarization processes are simple diffusion controlled. This conclusion is reached on the basis of certain observed facts which, in general, have been accepted as criteria for the validity of the diffusion rate theory. These are:

(a) Peripheral velocity has a remarkable effect on the dissolution rate. The rate constants are directly proportional to peripheral velocity to 0.98 power.

(b) The temperature coefficients are small compared to those of chemical reactions. Values of activation energies are well below 4 kcal per mole.

(c) There is a significant effect of turbulence near the metal surface.

(d) The dissolution rate is directly proportional to the surface area.

3. The experimental data obtained suggest that the autocatalytic reaction is still diffusion controlled. However, the autoxidation process which may occur at the metal surface may also be a slow step, and therefore plays an important role in the determination of rate control. The arguments in favor of this conclusion are:

(a) The dissolution rate is directly proportional to peripheral velocity to the powers of 0.30 and 0.90.

(b) The value of activation energy of 5.54 kcal per mole is a little larger than the 3-4 kcal per mole to be expected for a reaction under complete diffusion control.

(c) The effect of turbulence near the sample surface is significant.

(d) Dissolution rate is not directly proportional to the surface area A, but to the squre root of A.

4. Over the range 0.10-4.0 M HCl the dissolution rates are essentially independent of acid concentration.

5. The dependence of the dissolution rate on the square root of oxygen partial pressure is indicative of a dissociative adsorption of oxygen on the metal surface.

6. Formation of gray film on metal surface was observed. Other investigators have reported this film to be composed of pure tin.

7. The stannous species, stannic species equilibrium:

$$Sn + Sn_s^{++++} \rightleftarrows 2\,Sn_s^{++}$$

is assumed to be established at the metal surface.

APPENDIX I

POLAROGRAPHIC DETERMINATION OF TIN CONCENTRATION

A Sargent Model XV polarograph was used for the analysis of corroding solutions in this study.

A stock of 2×10^{-3} M tin ion solution was made by dissolving Analar Grade tin bars in 1 M HCl. Standard tin ion solutions were prepared by diluting aliquot samples of the stock solution with 1 M HCl. The dropping mercury electrode calibration curve (Figure 20) was made for a supporting electrolyte of 1 M HCl and 4 M NH_4Cl containing 0.005 per cent gelatin as suppressor.

The polarographic cell containing the corroding solution sample and the reference Calomel cell were immersed in a constant temperature bath at $25^{\circ}C$. Before each polarographic analysis the corroding solution sample was flushed with nitrogen gas for approximately 10 minutes. For high tin ion concentrations, solutions were diluted and a corresponding amount of gelatin and NH_4Cl were added.

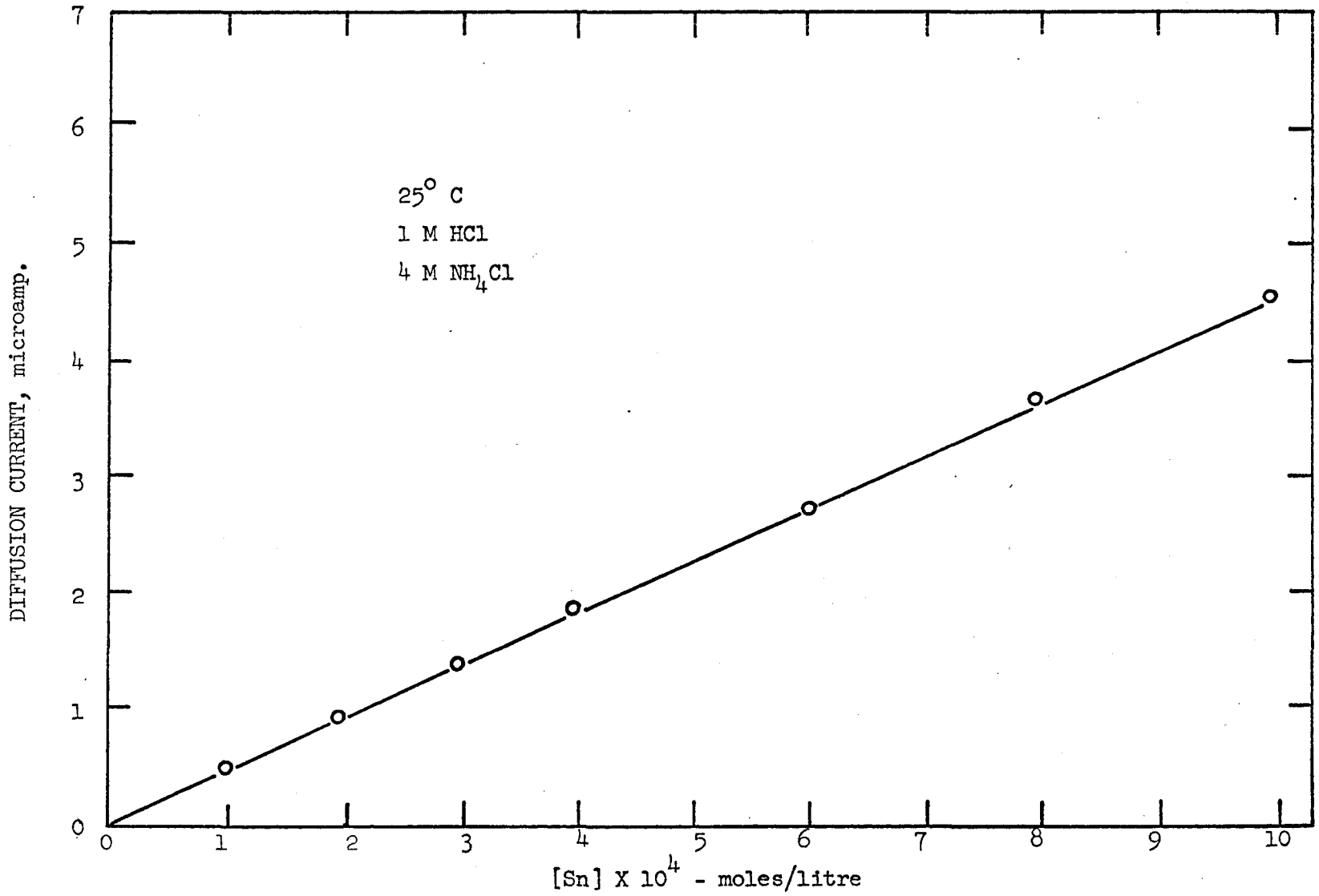

FIGURE 20. CALIBRATION CURVE
(Sargent Model XV polarograph)

APPENDIX II

DATA OF TIN DISSOLUTION

EFFECT OF PERIPHERAL VELOCITY

35° C
500 ml 1M HCl
3.66 sq.cm.
air

Run 1 - 2,840 cm./min.

Time (min.)	[Sn] mol./l.
20	0.25×10^{-4}
40	0.56
60	0.85
80	1.22
100	1.51
120	1.92
140	2.25

Run 2 - 3,400 cm./min.

Time (min.)	[Sn] mol./l.
20	0.30×10^{-4}
40	0.55
60	0.90
80	1.30
100	1.60
120	2.00
140	2.39

Run 3 - 8,500cm./min.

Time (min.)	[Sn] mol./l.
20	0.45×10^{-4}
40	0.98
60	1.45
80	1.92
100	2.45
120	3.00
140	3.60

Run 4 - 14,200 cm./min.

Time (min.)	[Sn] mol./l.
20	0.73×10^{-4}
40	1.46
60	2.31
80	3.30
100	4.20
120	5.25
140	6.20

Run 5 - 19,900 cm./min.

20	1.15×10^{-4}
40	2.46
60	3.71
80	5.11
100	6.42
120	7.81
140	9.25

Run 6 - 27,000 cm./min.

20	1.15×10^{-4}
40	2.61
60	3.80
80	5.40
100	7.21
120	9.25
140	11.40

Run 7 - 34,100 cm./min.

20	1.74×10^{-4}
40	3.75
60	6.21
80	8.62
100	11.31
120	13.71
140	17.10

EFFECT OF PERIPHERAL VELOCITY

25° C
500 ml 1M HCl
3.66 sq.cm.
air

Run 8 - 2,840 cm./min.

Time (min.)	[Sn] mol./l.
20	0.30×10^{-4}
40	0.65
60	0.95
80	1.41
100	1.71
120	2.12
140	2.62

Run 9 - 8,500 cm./min.

Time (min.)	[Sn] mol./l.
20	0.21×10^{-4}
40	0.44
60	0.73
80	1.04
100	1.41
120	1.80
140	2.22

Run 10 - 14,200cm./min.

Time (min.)	[Sn] mol./l.
20	0.45×10^{-4}
40	0.80
60	1.31
80	1.85
100	2.41
120	3.10
140	3.75

Run 11 - 19,900 cm./min.

Time (min.)	[Sn] mol./l.
20	0.81×10^{-4}
40	1.65
60	2.60
80	3.49
100	4.61
120	5.70
140	6.81

Run 12 - 27,000 cm./min.

20	0.92×10^{-4}
40	2.11
60	3.50
80	4.72
100	6.30
120	8.15
140	9.85

Run 13 - 34,100cm./min.

20	1.51×10^{-4}
40	3.40
60	5.51
80	7.49
100	9.81
120	12.51
140	15.02

EFFECT OF PERIPHERAL VELOCITY

500 ml 1M HCl
3.66 sq.cm.
Nitrogen

25° C

Run 14 - 8,500 cm./min.		Run 15 - 14,200cm./min.		Run 16 - 21,230 cm./min.		Run 17 - 34,100 cm./min.	
Time (min.)	[Sn] mol./l.	Time (min.)	[Sn] mol./l.	Time (min.)	[Sn] mol./l.	Time (min.)	[Sn] mol./l.
20	0.11×10^{-4}	20	0.10×10^{-4}	20	0.12×10^{-4}	20	0.14×10^{-4}
40	0.16	40	0.16	40	0.21	40	0.31
60	0.18	60	0.20	60	0.29	60	0.44
80	0.19	80	0.27	80	0.41	80	0.62
100	0.21	100	0.31	100	0.51	100	0.75
120	0.26	120	0.41	120	0.62	120	0.93
140	0.31	140	0.45	140	0.71	140	1.06

35° C

Run 18 - 8,500 cm./min.		Run 19 - 14,200 cm./min.		Run 20 - 21,230 cm./min.		Run 21 - 34,100 cm./min.	
20	0.10×10^{-4}	20	0.11×10^{-4}	20	0.13×10^{-4}	20	0.18×10^{-4}
40	0.13	40	0.17	40	0.24	40	0.38
60	0.16	60	0.24	60	0.38	60	0.52
80	0.20	80	0.29	80	0.45	80	0.75
100	0.26	100	0.40	100	0.61	100	0.87
120	0.29	120	0.44	120	0.69	120	1.06
140	0.34	140	0.52	140	0.81	140	1.24

EFFECT OF PERIPHERAL VELOCITY

500 ml 1M HCl
3.66 sq.cm.
Nitrogen
40° C

Run 22 - 8,500 cm./min		Run 23 - 14,200 cm./min.		Run 24 - 21,230 cm./min.		Run 25 - 34,100 cm./min.	
Time (min.)	[Sn] mol./l.	Time (min.)	[Sn] mol./l.	Time (min.)	[Sn] mol./l.	Time (min.)	[Sn] mol./l.
20	0.11×10^{-4}	20	0.11×10^{-4}	20	0.15×10^{-4}	20	0.21×10^{-4}
40	0.15	40	0.17	40	0.25	40	0.38
60	0.17	60	0.25	60	0.39	60	0.60
80	0.20	80	0.31	80	0.58	80	0.77
100	0.27	100	0.42	100	0.65	100	1.01
120	0.30	120	0.49	120	0.81	120	1.16
140	0.36	140	0.58	140	0.96	140	1.37

EFFECT OF TEMPERATURE VARIATION

34,100 cm./min.
500 ml 1M HCl
3.66 sq.cm.
Air

Run 26 - 25°C.

Time (min.)	[Sn] mol./l.
20	1.10×10^{-4}
40	2.50
60	4.18
80	5.95
100	7.45
120	9.41
140	11.20

Run 27 - 30°C.

Time (min.)	[Sn] mol./l.
20	1.43×10^{-4}
40	2.79
60	4.57
80	6.86
100	8.64
120	11.10
140	13.22

Run 28 - 35°C.

Time (min.)	[Sn] mol./l.
20	1.53×10^{-4}
40	2.82
60	4.75
80	7.35
100	9.51
120	12.42
140	15.10

Run 29 - 40°C.

Time (min.)	[Sn] mol./l.
20	1.29×10^{-4}
40	3.02
60	5.19
80	7.70
100	10.22
120	13.55
140	16.90

Run 30 - 45°C

20	1.49×10^{-4}
40	3.59
60	5.91
80	8.65
100	11.60
120	15.55
140	19.41

EFFECT OF TEMPERATURE VARIATION

34,100 cm./min.
500 ml 1M HCl
3.66 sq.cm.
Nitrogen

Run 31 - 25°C.

Time (min.)	[Sn] mol./l.
20	0.15×10^{-4}
40	0.28
60	0.42
80	0.60
100	0.74
120	0.91
140	1.06

Run 32 - 30°C.

Time (min.)	[Sn] mol./l.
20	0.17×10^{-4}
40	0.31
60	0.42
80	0.61
100	0.74
120	0.92
140	1.15

Run 33 - 35°C.

Time (min.)	[Sn] mol./l.
20	0.18×10^{-4}
40	0.35
60	0.55
80	0.69
100	0.91
120	1.05
140	1.25

Run 34 - 40°C.

Time (min.)	[Sn] mol./l.
20	0.18×10^{-4}
40	0.38
60	0.59
80	0.76
100	0.96
120	1.15
140	1.34

Run 35 - 45°C.

20	0.21×10^{-4}
40	0.41
60	0.64
80	0.85
100	1.04
120	1.28
140	1.47

VARIATION OF TEMPERATURE AND SAMPLE DIAMETER

34,100 cm./min.
500 ml 1M HCl
3.66 sq.cm.
$d = {}^{Air}1.07$ cm.

Run 36 - 25°C.

Time (min.)	[Sn] mol./l.
20	0.72×10^{-4}
40	1.72
60	3.30
80	5.31
100	7.34
120	9.81
140	12.11

Run 37 - 30°C.

Time (min.)	[Sn] mol./l.
20	0.79×10^{-4}
40	2.15
60	4.02
80	6.05
100	9.05
120	11.70
140	15.81

Run 38 - 35°C.

Time (min.)	[Sn] mol./l.
20	1.24×10^{-4}
40	2.92
60	5.54
80	8.31
100	11.71
120	15.98
140	20.81

Run 39 - 40°C.

Time (min.)	[Sn] mol./l.
20	1.14×10^{-4}
40	3.03
60	5.61
80	8.70
100	12.81
120	17.40
140	23.30

Run 40 - 45°C.

20	1.06×10^{-4}
40	3.03
60	6.01
80	9.30
100	14.00
120	20.11
140	26.71

VARIATION OF TEMPERATURE AND SAMPLE DIAMETER

34,100 cm./min.
500 ml 1M HCl
3.66 sq.cm.
Air
d = 1.37 cm.

Run 41 - 25°C.

Time (min.)	[Sn] mol./l.
20	1.49×10^{-4}
40	3.35
60	5.71
80	8.90
100	12.45
120	17.61
140	22.80

Run 42 - 30°C.

Time (min.)	[Sn] mol./l.
20	1.52×10^{-4}
40	3.41
60	6.20
80	9.68
100	14.21
120	20.25
140	26.40

Run 43 - 35°C.

Time (min.)	[Sn] mol./l.
20	1.88×10^{-4}
40	4.02
60	7.45
80	11.70
100	17.60
120	25.02
140	33.30

Run 44 - 40°C.

Time (min.)	[Sn] mol./l.
20	1.98×10^{-4}
40	4.45
60	7.95
80	12.30
100	18.91
120	28.00
140	38.51

Run 45 - 45°C.

20	2.11×10^{-4}
40	4.66
60	8.12
80	13.10
100	20.41
120	30.05
140	41.80

VARIATION OF TEMPERATURE AND SAMPLE DIAMETER

34,100 cm./min.
500 ml 1M HCl
3.66 sq.cm.
Air
d = 1.83 cm.

Run 46 - 25°C.

Time (min.)	[Sn] mol./l.
20	1.37×10^{-4}
40	3.06
60	5.48
80	9.02
100	13.75
120	19.01
140	25.62

Run 47 - 30°C.

Time (min.)	[Sn] mol./l.
20	1.72×10^{-4}
40	4.02
60	7.22
80	11.89
100	17.75
120	25.20
140	33.95

Run 48 - 35°C.

Time (min.)	[Sn] mol./l.
20	1.96×10^{-4}
40	4.16
60	7.68
80	11.15
100	19.90
120	27.95
140	38.21

Run 49 - 40°C.

Time (min.)	[Sn] mol./l.
20	2.01×10^{-4}
40	4.61
60	8.18
80	13.25
100	21.44
120	31.76
140	43.91

Run 50 - 45°C.

20	2.21×10^{-4}
40	4.85
60	8.47
80	13.55
100	22.96
120	34.56
140	48.92

VARIATION OF TEMPERATURE AND SAMPLE DIAMETER

34,100 cm./min.
500 ml 1M HCl
3.66 sq.cm.
Air
d = 2.41 cm.

Run 51 - 25°C.

Time (min.)	[Sn] mol./l.
20	0.865×10^{-4}
40	2.11
60	3.72
80	5.76
100	9.45
120	14.87
140	20.65

Run 52 - 30°C.

Time (min.)	[Sn] mol./l.
20	1.34×10^{-4}
40	3.06
60	5.15
80	8.41
100	13.65
120	20.89
140	28.80

Run 53 - 35°C.

Time (min.)	[Sn] mol./l.
20	1.98×10^{-4}
40	4.33
60	7.22
80	11.59
100	18.33
120	27.21
140	37.42

Run 54 - 40°C.

Time (min.)	[Sn] mol./l.
20	2.1×10^{-4}
40	4.32
60	7.61
80	12.21
100	19.95
120	31.42
140	43.69

Run 55 - 45°C.

20	1.93×10^{-4}
40	4.33
60	7.85
80	12.86
100	22.15
120	35.71
140	50.81

VARIATION OF SAMPLE DIAMETER

34,100 cm./min.
500 ml 1M HCl
3.66 sq.cm.
35°C.
Air

Run 56 - 0.915 cm.

Time (min.)	[Sn] mol./l.
20	2.17×10^{-4}
40	3.92
60	6.31
80	8.92
100	11.89
120	15.15
140	18.59

Run 57 - 1.07 cm.

Time (min.)	[Sn] mol./l.
20	2.28×10^{-4}
40	4.51
60	7.61
80	10.78
100	14.60
120	19.15
140	24.44

Run 58 - 1.22 cm.

Time (min.)	[Sn] mol./l.
20	2.70×10^{-4}
40	5.03
60	8.51
80	12.78
100	18.55
120	24.81
140	32.75

Run 59 - 1.37 cm.

Time (min.)	[Sn] mol./l.
20	3.92×10^{-4}
40	6.98
60	11.18
80	16.21
100	22.85
120	30.91
140	40.50

Run 60 - 1.52cm.

Time (min.)	[Sn] mol./l.
20	4.02×10^{-4}
40	7.45
60	11.41
80	16.19
100	24.30
120	32.71
140	43.75

Run 61 - 1.68 cm.

Time (min.)	[Sn] mol./l.
20	4.76×10^{-4}
40	8.41
60	12.95
80	18.96
100	27.65
120	36.55
140	49.44

Run 62 - 1.83 cm.

Time (min.)	[Sn] mol./l.
20	5.31×10^{-4}
40	8.89
60	13.55
80	20.09
100	28.56
120	38.86
140	50.31

Run 63 - 1.98 cm.

Time (min.)	[Sn] mol./l.
20	1.28×10^{-4}
40	3.27
60	6.01
80	10.61
100	16.41
120	24.78
140	34.55

VARIATION OF SAMPLE DIAMETER

34,100 cm./min.
500 ml 1M HCl
3.66 sq.cm.
35°C.
Air

Run 64 - 2.13 cm.

Time (min.)	[Sn] mol./l.
20	1.64×10^{-4}
40	4.01
60	7.11
80	11.14
100	18.15
120	26.96
140	36.88

Run 65 - 2.36 cm.

Time (min.)	[Sn] mol./l.
20	2.01×10^{-4}
40	4.53
60	7.61
80	12.22
100	19.15
120	28.33
140	38.96

Run 66 - 2.41 cm.

Time (min.)	[Sn] mol./l.
20	2.15×10^{-4}
40	4.65
60	7.95
80	12.98
100	20.41
120	29.70
140	40.95

VARIATION OF SAMPLE DIAMETER

34,100 cm./min.
500 ml 1M HCl
3.66 sq.cm.
35°C.
Nitrogen

Run 67 - 0.915 cm.

Time (min.)	[Sn] mol./l.
20	0.13×10^{-4}
40	0.35
60	0.49
80	0.68
100	0.85
120	1.06
140	1.27

Run 68 - 1.07 cm.

Time (min.)	[Sn] mol./l.
20	0.22×10^{-4}
40	0.49
60	0.71
80	0.98
100	1.22
120	1.41
140	1.70

Run 69 - 1.22 cm.

Time (min.)	[Sn] mol./l.
20	0.36×10^{-4}
40	0.60
60	0.91
80	1.31
100	1.60
120	1.91
140	2.24

Run 70 - 1.37 cm.

Time (min.)	[Sn] mol./l.
20	0.35×10^{-4}
40	0.71
60	1.01
80	1.35
100	1.76
120	2.01
140	2.38

Run 71 - 1.52 cm.

20	0.37×10^{-4}
40	0.79
60	1.06
80	1.42
100	1.77
120	2.09
140	2.49

Run 72 - 1.68 cm.

20	0.32×10^{-4}
40	0.69
60	1.05
80	1.30
100	1.69
120	2.09
140	2.41

Run 73 - 1.83 cm.

20	0.36×10^{-4}
40	0.79
60	1.11
80	1.46
100	1.84
120	2.18
140	2.52

Run 74 - 1.98 cm.

20	0.35×10^{-4}
40	0.73
60	1.07
80	1.44
100	1.79
120	2.18
140	2.54

VARIATION OF SAMPLE DIAMETER

34,100 cm./min.
500 ml 1M HCl
3.66 sq.cm.
35°C.
Nitrogen

Run 75 - 2.13 cm.

Time (min.)	[Sn] mol./l.
20	0.37×10^{-4}
40	0.78
60	1.12
80	1.50
100	1.86
120	2.26
140	2.63

Run 76 - 2.36 cm.

Time (min.)	[Sn] mol./l.
20	0.33×10^{-4}
40	0.68
60	1.04
80	1.35
100	1.71
120	2.08
140	2.49

Run 77 - 2.41 cm.

Time (min.)	[Sn] mol./l.
20	0.35×10^{-4}
40	0.75
60	1.09
80	1.45
100	1.81
120	2.20
140	2.59

VARIATION OF SAMPLE DIAMETER

34,100 cm./min.
500 ml 1M HCl
3.66 sq.cm.
35°C.
Oxygen

Run 78 - 0.915 cm.

Time (min.)	[Sn] mol./l.
20	4.31×10^{-4}
40	7.79
60	13.16
80	19.80
100	25.66
120	33.81
140	41.50

Run 79 - 1.07 cm.

Time (min.)	[Sn] mol./l.
20	4.29×10^{-4}
40	8.60
60	13.60
80	20.75
100	28.51
120	38.22
140	48.45

Run 80 - 1.22 cm.

Time (min.)	[Sn] mol./l.
20	4.40×10^{-4}
40	8.46
60	14.60
80	21.55
100	30.60
120	40.65
140	52.98

Run 81 - 1.37 cm.

Time (min.)	[Sn] mol./l.
20	2.54×10^{-4}
40	6.31
60	10.81
80	16.41
100	24.85
120	33.10
140	45.31

Run 82 - 1.52 cm.

Time (min.)	[Sn] mol./l.
20	2.82×10^{-4}
40	6.70
60	11.41
80	17.65
100	25.91
120	35.75
140	48.01

Run 83 - 1.68 cm.

Time (min.)	[Sn] mol./l.
20	3.80×10^{-4}
40	8.49
60	14.01
80	21.40
100	30.45
120	41.00
140	53.89

Run 84 - 1.83 cm.

Time (min.)	[Sn] mol./l.
20	4.24×10^{-4}
40	8.81
60	14.45
80	21.90
100	31.11
120	42.51
140	55.90

Run 85 - 1.89 cm.

Time (min.)	[Sn] mol./l.
20	2.52×10^{-4}
40	5.85
60	10.60
80	16.95
100	24.70
120	35.65
140	46.55

VARIATION OF SAMPLE DIAMETER

34,100 cm./min.
500 ml 1M HCl
3.66 sq.cm.
35°C.
Oxygen

Run 86 - 2.13 cm.

Time (min.)	[Sn] mol./l.
20	2.10×10^{-4}
40	5.24
60	9.89
80	16.20
100	23.81
120	33.90
140	45.95

Run 87 - 2.36 cm.

Time (min.)	[Sn] mol./l.
20	1.42×10^{-4}
40	4.08
60	8.10
80	13.71
100	20.90
120	29.85
140	41.00

Run 88 - 2.41 cm.

Time (min.)	[Sn] mol./l.
20	3.16×10^{-4}
40	7.11
60	12.20
80	19.45
100	27.95
120	38.45
140	50.89

APPENDIX III

NOMENCLATURE

A	Apparent surface area of specimen, $cm.^2$
E	Activation energy for tin dissolution, kcal./mole
M	An atom of metal
[M]	Concentration of metal ions, moles/litre
M^*	Active sites on metal surface
P_{O_2}	Partial pressure of oxygen, atm.
[Sn]	Concentration of tin ions, moles/litre
Sn^*	Active sites on a tin surface
T	Temperature, ^oK
V	Corroding solution volume, litre
d	Diameter of specimen, cm.
k_1	Reaction rate constant for hydrogen evolution
k_2	Reaction rate constant for oxygen depolarization
k_3	Reaction rate constant for autocatalytic reaction
t	Time, min.
v	Peripheral velocity, cm./min.

Subscripts

b	The bulk of corroding solution
i	Metal-solution interface
s	Metal surface

REFERENCES

1. Alwitt, R.S. and R.S. Kapner, J. Electrochem. Soc., 112, 207 (1965).
2. Berzelius, J.J., Ann. Chim. Phys., 87, 50 (1813).
3. Berzelius, J.J., Ann. Chim. Phys., 5, 149 (1817).
4. Bodner, J.J., M.A.Sc. Thesis, University of Windsor, (1964).
5. Britton, S.C. and D.G. Michael, J. Appl. Chem., 7, 349 (1957).
6. Bumbulis, J. and W.F. Graydon, J. Electrochem. Soc., 109, 1130 (1962).
7. Evans, M.G., J.T. Baxendale and G.S. Park, Trans. Faraday. Soc., 42, 155 (1946).
8. Gnyp, A.W., Ph.D. Thesis, University of Toronto, (1958).
9. Hagymas, G. and M. Quintin, J. Chim. Phys. et Phys.Chim. Biol., 61, 541 (1964).
10. Hoar, T.P., Trans. Faraday. Soc., 33, 1152 (1937).
11. Kagetsu, T.J. and W.F. Graydon, J. Electrochem. Soc., 110, 709 (1963).
12. Khitrov, V.A. and V.I. Shatalova, Tsvetn. Metal, 35, 95 (1962).
13. Kilpatrick, M. and J.H. Rushton, J. Phys. Chem., 38, 269 (1934).
14. Kohman, E.F. and N.H. Sanborn, Ind. Eng. Chem., 20, 1373 (1928).
15. Krasil'shchikov, J. Phys. Chem. U.S.S.R., 14, 320 (1940).
16. Latimer, W., The Oxidation States of the Elements and Their Potentials in Aqueous Solutions, 2nd Ed., Prentice-Hall Book CO., Inc., Englewood Cliffs, N.J., (1952).
17. Levich, V.G., Physicochemical Hydrodynamics, Prentice-Hall Book Co., Inc., Englewood Cliffs, N.J., (1962).
18. Lingane, J.J., J. Am. Chem. Soc., 67, 919 (1945).
19. Lingane, J.J., Chem. Rev., 29, 1-35 (1941).

REFERENCES (Contd.)

20. Lingane, J.J., Ind. Eng. Chem. Anal. Ed., 18, 429 (1946).

21. Lochman, S.J. and F.C. Tompkin, Trans. Faraday Soc., 40, 130 (1944).

22. Lu, B.C-Y. and W.F. Graydon, J. Am. Chem. Soc., 77, 6136 (1955).

23. Lu, B.C-Y. and W.F. Graydon, Can. J. Chem., 32, 153 (1954).

24. Lui, A.W.K., Ph.D. Thesis, University of Windsor, (1964).

25. Marshakov, I.K., Ya.A. Ugai and V.I. Vigdorovich, J. Appl. Chem. U.S.S.R., 38, 1101 (1965).

26. Nernst, H.W., Z. Phys. Chem., 47, 55 (1904).

27. Shchukorev, A.N., Phys. Chem. U.S.S.R., 28, 604 (1896).

28. Tomashov, N.D., Theory of Corrosion and Protection of Metals, The MacMillam Book Co., New York, (1966).

29. Weeks, J.R. and G.R. Hill, J. Electrochem. Soc., 103, 203 (1956).

30. Whitman, W.G. and R.P. Russel, J. Ind. Chem., 17, 348 (1925).